[29] E. J. Baerends, D. E. Ellis, and P. Ros, Chem. Phys. **2**, 41 (1973).
[30] K. Krijn and E. J. Baerends, *Fit Functions in the HFS-Method*, Internal Report, Free Unversity of Amsterdam, The Netherlands, 1984.
[31] P. M. Boerritger, G. te Velde, and E. J. Baerends, Int. J. Quantum Chem. **33**, 87 (1988); G. te Velde and E. J. Baerends, J. Comput. Phys. **99**, 84 (1992).
[32] L. Fan and T. Ziegler, J. Chem. Phys. **95**, 7401 (1991).
[33] D. P. Chong and S. R. Langhoff, J. Chem. Phys. **84**, 5606 (1986). See also R. Ahlrichs, P. Scharf, and C. Ehrhardt, *ibid.* **82**, 890 (1985).
[34] K. Raghavachari, G. W. Trucks, J. A. Pople, and M. Head-Gordon, Chem. Phys. Lett. **157**, 479 (1989).
[35] J. A. Pople, M. Head-Gordon, and K. Raghavachari, J. Chem. Phys. **87**, 5968 (1987).
[36] MOLECULE-SWEDEN is an electronic structure program written by J. Almlöf, C. W. Bauschlicher, M. R. A. Blomberg, D. P. Chong, A. Heiberg, S. R. Langhoff, P.-Å. Malmqvist, A. P. Rendell, B. O. Ross, P. E. M. Siegbahn, and P. R. Taylor.
[37] ADF 1.1.4, Department of Theoretical Chemistry, Vrije Universtiteit, Amsterdam.
[38] R. F. W. Bader, *Atoms in Molecules. A Quantum Theory* (Clarendon, Oxford, 1990).
[39] M. Sodupe, V. Branchadell, and A. Oliva, J. Phys. Chem. **99**, 8567 (1995).
[40] The computed MP2(DF) geometrical parameters of NO_2^- are r(N–O) =1.283(1.287) Å and ∠ONO=115.7(115.4)°. The experimental values are 1.25±0.02 Å and 117.5°.[41]
[41] K. M. Ervin, J. Ho, and W. C. Lineberger, J. Chem. Phys. **92**, 5404 (1988).
[42] The computed MP2(DF) geometrical parameters of NO_2 are r(N–O) =1.221(1.213) Å and ∠ONO=133.2(133.7)°. The experimental values are 1.194 Å and 133.9°.[43]
[43] Y. Morino, M. Tawimoto, S. Saito, E. Hirota, R. Awata, and T. Tanaka, J. Mol. Spectrosc. **98**, 331 (1983).
[44] M. Böhme and G. Frenking, Chem. Phys. Lett. **224**, 195 (1994).
[45] W. J. Lafferty and R. L. Sams, J. Mol. Spectrosc. **66**, 478 (1977).
[46] R. E. Watson and T. F. Brodasky, J. Chem. Phys. **27**, 683 (1957).

4. "Comparison of Density Functional and Coupled Cluster Methods in the Study of Metal-Ligand Systems: $ScCO_2$ and $CuNO_2$"

Comparison of density functional and coupled cluster methods in the study of metal–ligand systems: Sc–CO_2 and Cu–NO_2

Luis Rodríguez-Santiago, Mariona Sodupe, and Vicenç Branchadell
Departament de Química, Universitat Autònoma de Barcelona, Edifici Cn, 08193 Bellaterra, Spain

(Received 17 May 1996; accepted 5 September 1996)

The structure, binding energies, and vibrational frequencies have been determined for the $^1A_1$ state of the η^2-O,O coordination mode of Cu–NO_2 and the $^2A_1$ state of the η^2-O,O coordination mode of Sc–CO_2. Calculations have been done using coupled cluster methods and methods based on the density functional theory. The results obtained show that all the levels of calculation lead to very similar equilibrium geometries and vibrational frequencies, while different results are obtained for the binding energy. For Sc–CO_2 density functional methods overestimate the binding energy with respect to coupled cluster, while for Cu–NO_2 the density functional binding energies are lower than the coupled cluster value. In both cases the inclusion of the exact Hartree–Fock exchange into the functional leads to an improvement of the density functional result. Our best estimates for the binding energies of Sc–CO_2 and Cu–NO_2 are 25 and 50 kcal mol^{-1}, respectively. © *1996 American Institute of Physics.* [S0021-9606(96)01046-X]

INTRODUCTION

The study of metal–monoligand systems is of great interest, since it provides the most simple model for metal–ligand interactions. We have recently studied the complexes Sc–CO_2 (Ref. 1) and Cu–NO_2 (Ref. 2) using density functional methods in the geometry optimizations and frequencies calculations, while the binding energies have been calculated at higher levels of calculation.

In the last years, density functional methods[3] have been extensively used in the study of systems containing transition metals, yielding high quality results at a relatively low computational cost.[4] However, the same level of accuracy is not generally achieved in the study of metal–monoligand systems. Recent work in this area[5–21] has shown that, as a general trend, density functional methods yield reasonable molecular geometries and vibrational frequencies, but tend to overestimate binding energies. This fact has been related to the incorrect representation of atomic states arising from different electronic configurations of the metal.[8,9] This overbinding is partially corrected when hybrid functionals, that incorporate contributions from the exact Hartree–Fock exchange, are used.[10,11,14,15,17,22] On the other hand, our study of Cu–NO_2 (Ref. 2) has shown that the binding energy computed at the density functional level is smaller than the values obtained using conventional *ab initio* methods.

The purpose of the present paper is to study the Sc–CO_2 and Cu–NO_2 systems using different functionals in order to assess their validity in the study of geometries, vibrational frequencies, and binding energies. For this reason, the results provided by the different functionals will be compared with those obtained from high level conventional *ab initio* calculations.

COMPUTATIONAL DETAILS

Density functional (DF) calculations have been done using the two different gradient-corrected functionals: The exchange functional of Becke[23] with the correlation functional of Perdew[24] (B–P), and the same exchange functional along with the correlation functional of Lee, Yang, and Parr[25] (B–LYP). Moreover, the LYP exchange functional has also been used with two different hybrid exchange functionals: Becke's half and half[26] (BH–LYP) and Becke's three parameter functional[27] (B3–LYP). Conventional *ab initio* calculations have been carried out at the coupled cluster with single and double excitations level, with a perturbative estimate of the triple excitations [CCSD(T)].[28] Molecular geometries and harmonic vibrational frequencies have been determined at all these levels of calculation. In the geometry optimization at the CCSD(T) level of calculation we have correlated all electrons of N, C, and O except the $1s$. For Sc and Cu we have correlated the $3d$ and $4s$ electrons. In the calculation of the binding energy of Sc–CO_2 we have also correlated the $3s$ and $3p$ electrons, since the correlation has a noticeable effect on the computed values (about 5.0 kcal mol^{-1}). For Cu–NO_2 we have observed that this effect is negligible (about 0.1 kcal mol^{-1}).

The same basis set has been used in all these calculations. The Cu and Sc basis set is a $[8s4p3d]$ contraction of the $(14s9p5d)$ primitive set of Wachters[29] supplemented with two diffuse p and one diffuse d functions.[30] The final basis set is of the form $(14s11p6d)/[8s6p4d]$. For C, N, and O we use the $(9s5p)/[4s2p]$ set developed by Dunning,[31] supplemented with a valence diffuse function ($\alpha_{sp}=0.0438$ for carbon, $\alpha_{sp}=0.0639$ for nitrogen, and $\alpha_{sp}=0.0845$ for oxygen) and one 3d polarization function ($\alpha=0.75$ for carbon, $\alpha=0.80$ for nitrogen, and $\alpha=0.85$ for oxygen). This basis set is referred to as $D95+*$ in the GAUSSIAN 94[32] program system.

We have also carried out single point calculations using a larger basis set. In these calculations the metal basis set is further augmented by a single contracted set of f polarization functions that is based on a three-term fit to a Slater-type orbital, which leads to a $(14s11p6d3f)/[8s6p4d1f]$ basis

 0021-9606/96/105(22)/9966/6/$10.00

TABLE I. Optimized geometry parameters of $Sc-CO_2$ and $Cu-NO_2$ computed at several levels of calculation. [a]

Level of calc.	r(M–O)	r(X–O)	A(OXO)
$Sc-CO_2$			
B–P	1.927(−0.018)	1.372(−0.008)	111.7(1.4)
B–LYP	1.945(0.000)	1.375(−0.005)	111.3(1.0)
B3–LYP	1.928(−0.017)	1.358(−0.022)	110.8(0.5)
BH–LYP	1.918(−0.027)	1.342(−0.038)	110.0(−0.3)
CCSD(T)	1.945	1.380	110.3
$Cu-NO_2$			
B–P	2.086(−0.007)	1.276(−0.006)	114.3(0.9)
B–LYP	2.112(0.019)	1.283(0.001)	114.3(0.9)
B3–LYP	2.090(−0.003)	1.264(−0.018)	114.2(0.8)
BH–LYP	2.077(−0.016)	1.245(−0.037)	114.0(0.6)
CCSD(T)	2.093	1.282	113.4

[a]Bond lengths are in angstroms and angles in degrees. In parentheses values relative to CCSD(T).

set.[33] For C, N, and O we have used a $(10s5p2d1f)/[4s3p2d1f]$ basis set augmented with one diffuse s and one diffuse p functions.[34] This basis set, augmented with one diffuse d and one diffuse f functions, is referred to as aug-cc-pVTZ in the GAUSSIAN 94 program.[32]

All these calculations have been done using the GAUSSIAN 94 program.[32] For $Sc-CO_2$ we have also performed calculations with the modified coupled pair functional method (MCPF)[35] implemented in the MOLECULE-SWEDEN program.[36]

RESULTS AND DISCUSSION

The geometries of the $Sc-CO_2$ and $Cu-NO_2$ complexes are schematically represented in Chart 1.

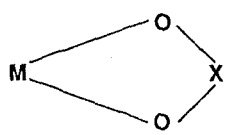

They correspond to the most stable structures obtained in our previous work.[1,2] Table I presents the geometries of $Sc-CO_2$ and $Cu-NO_2$ optimized at several levels of calculation. For both complexes, we have taken as reference the geometry parameters obtained at the CCSD(T) level of calculation. Table I shows that in all cases, DF geometries are very close to the ones obtained at the highest level of calculation. Regarding the bond lengths, the maximum deviation is produced for the X–O bond at the BH–LYP level: −0.038 Å for $Sc-CO_2$ (2.8% deviation) and −0.037 Å for $Cu-NO_2$ (2.9% deviation). With respect to bond angles, the largest deviation is produced in the OCO angle of $Sc-CO_2$ at the B–P level: 1.4° (1.3% deviation). DF bonds are generally shorter than the CCSD(T) ones, except for the B–LYP functional. B–P, B–LYP, and B3–LYP yield results in closer agreement with CCSD(T) than BH–LYP.

The harmonic vibrational frequencies computed for $Sc-CO_2$ and $Cu-NO_2$ are presented in Table II. Let us first consider the frequencies of the $Cu-NO_2$ complex. We can observe that, in general, the B–P and B–LYP functionals yield frequencies lower than the ones obtained at the CCSD(T) level, the only exception being the b_1 wagging vibration for both functionals and the b_2 asymmetric N–O stretching for B–P. The inclusion of Hartree–Fock exchange

TABLE II. Harmonic vibrational frequencies of $Sc-CO_2$ and $Cu-NO_2$ computed at several levels of calculation. [a]

Level of calc.	$M-XO_2$ in-plane wag (b_2)	$M-XO_2$ out-of-plane wag(b_1)	$M-XO_2$ stretch (a_1)	XO_2 bend (a_1)	XO stretch (b_2)	XO stretch (a_1)
$Cu-NO_2$						
B–P	160(−51)	382(47)	311(−13)	840(−11)	1280(7)	1228(−54)
B–LYP	132(−79)	378(43)	296(−28)	826(−25)	1228(−45)	1194(−88)
B3–LYP	187(−24)	373(38)	319(−5)	874(23)	1335(62)	1311(29)
BH–LYP	220(9)	360(25)	337(13)	926(75)	1437(164)	1445(163)
CCSD(T)	211	335	324	851	1273	1282
$Sc-CO_2$						
B–P	371	312	479	750	942	998
B–LYP	347	312	463	740	912	977
B3–LYP	387	314	483	776	983	1054
BH–LYP	432	313	502	820	1057	1146

[a]In cm^{-1}. In parentheses values relative to CCSD(T).

TABLE III. Bond dissociation energies of $Cu-NO_2$ and $Sc-CO_2$ computed at several levels of calculation.

	D_e[a]	
Level of calc.	$Sc-CO_2$	$Cu-NO_2$
B–P	40.9(+21.0)	49.5(−7.8)
B–LYP	37.3(+17.4)	47.8(−9.5)
B3–LYP	29.4(+9.5)	49.2(−8.1)
BH–LYP	17.3(−2.6)	52.1(−5.2)
CCSD(T)	19.9(0.0)	57.3(0.0)

[a]In kcal mol^{-1}. In parentheses values relative to CCSD(T).

TABLE IV. First ionization energy[a] of Sc and Cu computed at several levels of calculation.

	E_I	
Level of calc.	Sc	Cu
B–P	6.436(+0.143)	8.285(+1.124)
B–LYP	6.358(+0.065)	8.189(+1.128)
B3–LYP	6.490(+0.197)	8.030(+0.969)
BH–LYP	6.333(+0.040)	7.502(+0.441)
CCSD (T)	6.293(0.0)	7.061(0.0)
Expt.	6.54[b]	7.726[b]

[a]In eV. In parentheses values relative to CCSD(T).
[b]Reference 40.

in the functional produces an increase in the values of all computed frequencies except the b_1 wagging. With the B3–LYP functional most of the frequencies are larger than the corresponding CCSD(T) ones, while BH–LYP frequencies are always larger than the B3–LYP ones. There is a variation in the ordering of the two N–O stretching frequencies. According to all the functionals except BH–LYP the asymmetric N–O stretching vibration appears at a higher frequency than the symmetric stretching, as in NO_2.[37] On the other hand, the ordering is inverted in the BH–LYP and CCSD(T) calculations, leading to the same ordering observed in NO_2^-.[38]

In spite of reproducing the CCSD(T) ordering, the BH–LYP N–O stretching frequencies are too large, with an error relative to CCSD(T) of about twice the error produced by the other functionals. The asymmetric N–O stretching frequency computed at the CCSD(T) level is only 53 cm^{-1} larger than the experimental value of 1220 cm^{-1}.[39]

As a summary of this comparison between DF and CCSD(T) frequencies, we can say that all functionals, except BH–LYP, yield frequencies within less than 100 cm^{-1} of the CCSD(T) ones. Regarding the frequencies of $Sc-CO_2$, we obtain very similar results with the first three functionals, while BH–LYP frequencies are generally larger. According to the results obtained for $Cu-NO_2$, we expect the BH–LYP results to be less accurate than the results obtained using the other functionals.

The bond dissociation energies computed for the $Cu-NO_2$ and $Sc-CO_2$ complexes are presented in Table III. If we take the CCSD(T) values as the reference, we can see that DF calculations on $Sc-CO_2$ and $Cu-NO_2$ have different behavior. For $Sc-CO_2$ all DF methods except BH–LYP overestimate the binding energy, while for $Cu-NO_2$ the DF binding energies are lower than the CCSD(T) value. When comparing the different functionals, in all cases, BH–LYP yields the best result, i.e., the closest to CCSD(T). By comparing the three calculations that only differ in the exchange functional (B–LYP, B3–LYP, and BH–LYP), one can observe that the inclusion of the exact HF exchange into the functional leads to an improvement of the result, this being specially important for $Sc-CO_2$. As the contribution of exact exchange increases, the computed binding energies approach the CCSD(T) values.

The different behavior of $Sc-CO_2$ and $Cu-NO_2$ when changing the exchange functional shows that DF calculations overestimate the stabilizing contribution of exchange in the $Sc-CO_2$ complex with respect to the fragments. On the contrary, for $Cu-NO_2$ the stabilizing contribution of exchange is overestimated in the fragments. This tendency has also been observed in pilot calculations in which we have computed the binding energies at the HF level (exact exchange) and the DF level, using the Becke's exchange potential and no correlation potential (B-null).

We have shown in our previous studies[1,2] that both complexes have an important ionic character. According to this fact, the different behavior of the DF and CCSD(T) methods should be related to the computed values of the first ionization energy of the metal and of the electron affinity of the ligand. Tables IV and V present, respectively, the computed values of first ionization energies and adiabatic electron affinities.

For the first ionization energy of Sc, all theoretical results are lower than the experimental value. CCSD(T) provides the lowest value, 0.25 eV below the experimental one. The inclusion of exact exchange in the DF calculations does not show any systematic variation when the results are compared with CCSD(T). Regarding the first ionization energy of Cu, Table IV shows that CCSD(T) underestimates it by almost 0.7 eV. DF calculations with no hybrid functionals yield first ionization energies higher than the experimental value. The inclusion of exact exchange leads to a systematic lowering of the computed values, approaching the CCSD(T) result.

TABLE V. Adiabatic electron affinities[a] of CO_2 and NO_2 computed at several levels of calculation.

	E_{ea}	
Level of calc.	CO_2	NO_2
B–P	−0.241(+0.485)	2.217(+0.115)
B–LYP	−0.322(+0.404)	2.159(+0.057)
B3–LYP	−0.259(+0.467)	2.356(+0.254)
BH–LYP	−0.458(+0.268)	2.291(+0.189)
CCSD(T)	−0.726(0.0)	2.102(0.0)
Expt.	−0.6[b]	2.28[c]

[a]In eV. In parentheses values relative to CCSD(T).
[b]Reference 41.
[c]Reference 42.

TABLE VI. Energy of formation of the M^+ and L^- ions from M and L [a] computed at several levels of calculation.

Level of calc.	Sc–CO_2	Cu–NO_2
B–P	6.677(−0.342)	6.068(+1.109)
B–LYP	6.680(−0.339)	6.030(+1.071)
B3–LYP	6.749(−0.270)	5.674(+0.715)
HB–LYP	6.791(−0.228)	5.211(+0.252)
CCSD(T)	7.019(0.0)	4.959(0.0)
Expt.	7.1[b]	5.45[c]

[a]$\Delta E_1 = E_I(M) - E_{ea}(L)$, in eV. In parentheses values relative to CCSD(T).
[b]References 40 and 41.
[c]References 40 and 42.

The first ionization energy of Sc is reasonably well represented by all the theoretical levels, so that this factor does not explain the different values of the binding energy of Sc–CO_2. On the other hand, the computed values of the first ionization energy of Cu vary within a range of 1.2 eV. DF calculations tend to overestimate the first ionization energy of Cu, while CCSD(T) underestimates it. These results are in good agreement with the fact that CCSD(T) binding energy is larger than any of the values computed using DF.

The different accuracy of DF methods in the determination of the first ionization energies of the first row transition metals has already been discussed by several authors.[8,43,44] Ziegler and Li[8] have rationalized the results in terms of the overestimation by the current exchange functionals of the $s-d$ exchange–correlation energy contribution due to electrons of the same spin. This term is absent in the Sc ($4s^2 3d^1$) to Sc^+ ($4s^1 3d^1$) ionization, while it is important for Cu. The fact that the inclusion of exact exchange in the DF calculations leads to lower values of the first ionization energy of Cu confirms this analysis.

Let us now consider the electron affinities of the ligands. Table V shows that CCSD(T) underestimates the adiabatic electron affinities of CO_2 and NO_2 by 0.1 and 0.2 eV, respectively. B–P and B–LYP calculations overestimate the electron affinity of CO_2 by 0.4–0.5 eV, while the values corresponding to NO_2 are very reasonable. The inclusion of exact exchange does not lead to any systematic improvement, although for CO_2, the BH–LYP result is clearly closer to the experimental value than any other of the DF results. The computed value of the electron affinity of CO_2 would be very sensitive to the choice of the exponent of the most diffuse basis functions. As these functions become more diffuse, the computed value would approach zero. We have used the standard exponents implemented in the GAUSSIAN 94 program[32] both for C and O and our computed electron affinities are only used to interpret the variation of the binding energy of Sc–CO_2 with the level of calculation.

The formation of a complex of essentially ionic nature between a metal M and a ligand L can be conceptually decomposed in two steps. The first one consists on the formation of the M^+ and L^- ions. In the second step both ions interact to yield the complex. The energy associated with the first step would be $E_I(M) - E_{ea}(L)$. This term will be referred to as ΔE_1. Table VI presents the values of this term computed for Sc–CO_2 and Cu–NO_2.

For Sc–CO_2, the CCSD(T) value of ΔE_1 is in very good agreement with the experimental result, while the DF calculations lead to lower values, due to the overestimation of the electron affinity of CO_2 (see Table V). The inclusion of exact exchange in the functional leads to results in closer agreement with CCSD(T).

Regarding Cu–NO_2, CCSD(T) underestimates ΔE_1 by 0.5 eV. This is mainly due to the underestimation of the first ionization energy of Cu (see Table IV). DF calculations lead to considerably larger values of this term, due to the overestimation of the first ionization energy. The use of hybrid functionals approaches the DF results to the CCSD(T) one.

The variation of ΔE_1 with the level of calculation qualitatively agrees with the variation of the values of the computed binding energies (see Table III). For Sc–CO_2 the DF calculations yield binding energies larger than the CCSD(T) value and for Cu–NO_2 the DF values are lower than the CCSD(T) one. However, while the computed binding energies differ by more than 20 kcal mol^{-1} for Sc–CO_2 and by less than 10 kcal mol^{-1} for Cu–NO_2 (see Table III), the differences in ΔE_1 are less than 10 kcal mol^{-1} for Sc–CO_2 and more than 25 kcal mol^{-1} for Cu–NO_2, so that there is another factor that has to be taken into account.

The ionization of Sc leads to Sc^+ with a ground state electronic configuration $3d^1\ 4s^1$. The $3d$ electron is the one that participates in the bonding with CO_2, while the $4s$ electron remains in the metal. In order to minimize the repulsion with the incoming ligand, this electron has to polarize away from the ligand through sd hybridation. The energetic cost of this polarization can be related to the $3d-4s$ promotion energy of Sc^+. Several authors have computed this promotion energy using both DF[8,14,15,17,44,45] and conventional *ab initio* methods.[46] These studies show that DF methods generally underestimate this promotion energy. This fact can be attributed to the tendency of the current exchange functionals to overbind d electrons.[8,44] The use of hybrid exchange functionals partially corrects this underestimation.[14,15,17] On the other hand, conventional *ab initio* methods tend to overestimate this promotion energy.[46] The difference between the value computed by Russo *et al.*[44] at the BLYP level (0.18 eV) and the QCISD(T) value reported by Raghavachari and Trucks[46] (1.12 eV), with basis sets of similar quality, is more than 20 kcal mol^{-1}. This fact may play a role in the difference between the values of the binding energy of Sc–CO_2 computed using density functional and CCSD(T) methods. This polarization, related to a $4s-3d$ promotion, is absent in Cu–NO_2, since Cu^+ has no s electron and the $3d$ shell is full.

Up to now we have compared the results obtained at several levels of calculation using in all cases the same basis set. We will now discuss the basis set effect on the computed binding energies. Table VII presents the values of the binding energies of Sc–CO_2 and Cu–NO_2 computed using the larger basis set.

For Sc–CO_2 the use of a larger basis set produces a diminution of the computed binding energy in all DF calculations (see Table III for comparison). This result can be

TABLE VII. Bond dissociation energies of $Cu-NO_2$ and $Sc-CO_2$ computed with the large basis set. [a]

	D_e [b]	
Level of calc.	$Sc-CO_2$	$Cu-NO_2$
B–LYP	33.1(+8.9)	45.3(−10.4)
B3–LYP	25.9(+1.7)	46.3(−9.4)
BH–LYP	14.1(−10.1)	48.8(−6.9)
CCSD(T)		55.7(0.0)
MCPF	24.2(0.0)	

[a] $[5s4p2d1f]$ basis set for C, N, and O and $[8s6p4d1f]$ basis set for the metal.

[b] In kcal mol^{-1}. In parentheses values relative to MCPF for $Sc-CO_2$ and CCSD(T) for $Cu-NO_2$.

related to the variation of the ΔE_1 term when going from the smaller to the larger basis set. This term increases by 0.15 eV due to a diminution of the computed electron affinity of CO_2. The CCSD(T) calculation using the larger basis set has not been possible, so that we have examined the basis set effect at the MCPF level. This level of calculation gives a binding energy of 18.7 kcal mol^{-1} with the smaller basis set, very similar to the CCSD(T) value of 19.9 kcal mol^{-1} (see Table III). The value of the binding energy computed at the MCPF level with the larger basis set is 5.5 kcal mol^{-1} larger than the value corresponding to the smaller basis set. When going from the smaller to the larger basis set, ΔE_1 increases by 0.13 eV at the MCPF level, so that one could expect a decrease in the computed binding energy. However, the computed value increases. This result can be related to the diminution of the $s-d$ promotion energy computed by Raghavachari and Trucks[46] at the QCISD(T) level for Sc^+ using a basis set without f functions (1.2 eV) and with f functions (0.69 eV).

If we assume that the difference between MCPF and CCSD(T) binding energies computed with the larger basis would be about the same as the one calculated with the smaller basis set, we could predict the CCSD(T) binding energy with the larger basis set would be about 25 kcal mol^{-1}. This value is very similar to the one obtained at the B3–LYP level. On the other hand, the value obtained at the BH–LYP level is much lower, while this functional lead to the closest value to CCSD(T) with the smaller basis set (see Table III). The fact that with the larger basis set the DF (B3–LYP) and CCSD(T) values seem to converge to similar values leads us to conclude that our best estimate for the binding energy of $Sc-CO_2$ is 25 kcal mol^{-1}. This value is somewhat larger than our previous result of 17 kcal mol^{-1}.[1] The difference between both results is due to the fact that in the previous calculation the $3s$ and $3p$ electrons of Sc were not correlated.

For $Cu-NO_2$, the basis set effect is smaller than for $Sc-CO_2$. The use of a larger basis set produces the same effect on the computed binding energy at all levels of calculation, so that the difference between the DF and CCSD(T) results does not change. The functional that leads to the closest result to CCSD(T) is BH–LYP, as it was the case with the smaller basis set (see Table III). The value of the first ionization energy of Cu with the larger basis set is 7.16 eV, very similar to the value obtained with the smaller basis set, and notably smaller than the experimental value (see Table IV). Values closer to the experiment are obtained only with larger basis sets.[46] According to this fact, we expect the value of the binding energy of $Cu-NO_2$ computed at the CCSD(T) level with our larger basis set to be slightly overestimated. On the other hand, the value of the ionization potential of Cu computed at the BH–LYP level seems to indicate that the binding energy would be slightly underestimated at this level of calculation. According to these considerations one would expect that the correct value lie between the BH–LYP and the CCSD(T) values, so that our best estimate for this binding energy is about 50 kcal/mol.

CONCLUDING REMARKS

The structure, binding energy, and vibrational frequencies of $Sc-CO_2$ and $Cu-NO_2$ have been determined using density functional and coupled cluster methods. All levels of calculation lead to very similar equilibrium geometries and vibrational frequencies, while different results are obtained for the binding energy. In $Sc-CO_2$, density functional methods overestimate the binding energy with respect to the CCSD(T) value. On the contrary, for $Cu-NO_2$, the binding energy computed using density functional methods is always lower than the CCSD(T) value. In both cases, the introduction of exact exchange in the functional lowers the difference between the DF and CCSD(T) computed binding energies. The different behavior of both systems on the level of calculation has been rationalized in terms of two contributions. The first one is the difference between the first ionization energy of the metal and the electron affinity of the ligand involved in the formation of complexes with an important ionic character. This factor is determinant in $Cu-NO_2$, since the first ionization energy of Cu is greatly overestimated by the nonhybrid density functionals. For $Sc-CO_2$ the discrepancy between DF and CCSD(T) results has also been attributed to an underestimation of $4s-3d$ promotion energy in Sc^+ by the nonhybrid functionals. The use of hybrid exchange functionals partially corrects these deficiencies, but the development of new functionals seems necessary to obtain fully satisfactory results.

ACKNOWLEDGMENTS

This work has been financially supported by DGICYT (PB92-0621) and CIRIT (GRQ93-2079). Computer time from the Centre de Supercomputació de Catalunya (CESCA) and Centre Europeu de Paral.lelisme de Barcelona (CEPBA) is gratefully acknowledged. L.R. gratefully acknowledges the Spanish Ministry of Education and Science for a doctoral fellowship.

[1] M. Sodupe, V. Branchadell, and A. Oliva, J. Phys. Chem. **99**, 8567 (1995).

[2] L. Rodríguez-Santiago, V. Branchadell, and M. Sodupe, J. Chem. Phys. **103**, 9738 (1995).

[3] R. G. Parr and W. Yang, *Density Functional Theory of Atoms and Molecules* (Oxford University Press, New York, 1989).

[4] T. Ziegler, Chem. Rev. **91**, 651 (1991).
[5] R. Fournier, J. Chem. Phys. **98**, 8041 (1993).
[6] R. Fournier, J. Chem. Phys. **99**, 1801 (1993).
[7] I. Pápai, J. Mink, R. Fournier, and D. R. Salahub, J. Phys. Chem. **97**, 9986 (1993).
[8] T. Ziegler and J. Li, Can. J. Chem. **72**, 783 (1994).
[9] M. Castro, D. R. Salahub, and R. Fournier, J. Chem. Phys. **100**, 8233 (1994).
[10] V. Barone, Chem. Phys. Lett. **233**, 129 (1995).
[11] A. Ricca and C. W. Bauschlicher, Theor. Chim. Acta **92**, 123 (1995).
[12] C. W. Bauschlicher and P. Maitre, J. Phys. Chem. **99**, 3444 (1995).
[13] P. Maitre and C. W. Bauschlicher, J. Phys. Chem. **99**, 6836 (1995).
[14] M. C. Holthausen, C. Heinemann, H. H. Cornehl, W. Koch, and H. Schwarz, J. Chem. Phys. **102**, 4931 (1995).
[15] M. C. Holthausen, M. Mohr, and W. Koch, Chem. Phys. Lett. **240**, 245 (1995).
[16] I. Pápai, J. Chem. Phys. **103**, 1860 (1995).
[17] A. Ricca and C. W. Bauschlicher, Chem. Phys. Lett. **245**, 150 (1995).
[18] R. Fournier and I. Pápai, *Recent Advances in Density Functional Methods*, Vol. 3 Applications, edited by D. Chong (World Scientific, Singapore, 1995).
[19] S. C. Chung, S. Krüger, G. Pacchioni, and N. Rösch, J. Chem. Phys. **102**, 3695 (1995).
[20] J. Terra and D. Guenzburger, J. Phys. Chem. **99**, 4935 (1995).
[21] S. C. Chung, S. Krüger, S. P. Ruzankin, G. Pacchioni, and N. Rösch, Chem. Phys. Lett. **248**, 109 (1996).
[22] V. Barone and C. Adamo, J. Phys. Chem. **100**, 2094 (1996).
[23] A. D. Becke, Phys. Rev. A **38**, 3098 (1988).
[24] J. P. Perdew, Phys. Rev. B **33**, 8822 (1986).
[25] C. Lee, W. Yang, and R. G. Parr, Phys. Rev. B **37**, 785 (1988).
[26] A. D. Becke, J. Chem. Phys. **98**, 1372 (1993).
[27] A. D. Becke, J. Chem. Phys. **98**, 5648 (1993).
[28] K. Raghavachari, G. W. Trucks, J. A. Pople, and M. Head-Gordon, Chem. Phys. Lett. **157**, 479 (1989).
[29] A. J. H. Wachters, J. Chem. Phys. **52**, 1033 (1970).
[30] P. J. Hay, J. Chem. Phys. **66**, 4377 (1977).
[31] T. H. Dunning, J. Chem. Phys. **53**, 2823 (1970).
[32] GAUSSIAN 94, M. J. Frisch, G. W. Trucks, H. B. Schlegel, P. M. W. Gill, B. G. Johnson, M. A. Robb, J. R. Cheesman, T. A. Keith, G. A. Petersson, J. A. Montgomery, K. Raghavachari, M. A. Al-Laham, V. G. Zakrzewsky, J. V. Ortiz, J. B. Foresman, J. Cioslowsky, B. Stefanov, A. Nanayakkara, M. Challacombe, C. Y. Peng, P. Y. Ayala, W. Chen, M. W. Wong, J. L. Andrés, E. S. Replogle, R. Gomperts, R. L. Martin, D. J. Fox, J. S. Binkley, D. J. Defrees, J. Baker, J. J. P. Stewart, M. Head-Gordon, C. Gonzales, and J. A. Pople (Gaussian Inc., Pittsburgh, PA, 1995).
[33] R. F. Stewart, J. Chem. Phys. **52**, 431 (1970).
[34] R. A. Kendall and T. H. Dunning, J. Chem. Phys. **96**, 6796 (1992).
[35] D. P. Chong and S. R. Langhoff, J. Chem. Phys. **84**, 5606 (1986). See also R. Alrichs, P. Scharf, and C. Ehrhardt, J. Chem. Phys. **82**, 890 (1984).
[36] SWEDEN-MOLECULE is an electronic structure program written by J. Almlöf, C. W. Bauschlicher, M. R. A. Blomberg, D. P. Chong, A. Heiberg, S. R. Langhoff, P.-Å. Malmqvist, A. P. Rendell, B. O. Ross, P. E. M. Siegbahn, and P. R. Taylor.
[37] W. J. Lafferty and R. L. Sams, J. Mol. Spectrosc. **66**, 478 (1977).
[38] R. E. Watson and T. F. Brodasky, J. Chem. Phys. **27**, 683 (1957).
[39] D. Worden and D. W. Ball, J. Phys. Chem. **96**, 7167 (1992).
[40] C. E. Moore, *Atomic Energy Levels*, Natl. Bur. Stand. Circ., U.S., No. **467** (U.S. GPO, Washington, DC, 1949).
[41] R. N. Compton, P. W. Reinhardt, and C. D. Cooper, J. Chem. Phys. **63**, 3821 (1975).
[42] B. M. Hughes, C. Lifschitz, and T. O. Tiernan, J. Chem. Phys. **59**, 3162 (1973).
[43] O. Gunnarsson and R. O. Jones, Phys. Rev. B **31**, 7588 (1985).
[44] T. V. Russo, R. L. Martin, and P. J. Hay, J. Chem. Phys. **101**, 7729 (1994).
[45] F. W. Kutzler and G. S. Painter, Phys. Rev. B **43**, 6865 (1991).
[46] K. Raghavachari and G. W. Trucks, J. Chem. Phys. **91**, 2457 (1989).

5. "Coordination of NO_2 to Alkaline-Earth Metals. A theoretical Study"

630 *J. Phys. Chem. A* **1998,** *102,* 630−635

Coordination of NO_2 to Alkaline-Earth Metals. A Theoretical Study

Luis Rodríguez-Santiago, Mariona Sodupe,* and Vicenç Branchadell*

Departament de Química, Universitat Autònoma de Barcelona, Edifici Cn, 08193 Bellaterra, Spain

Received: July 24, 1997; In Final Form: October 31, 1997[⊗]

The structure and harmonic vibrational frequencies have been determined for the alkaline-earth metal MNO_2 systems (M = Be, Mg, Ca, and Sr) using the B3LYP method. Binding energies have also been calculated using conventional ab initio methods, CCSD(T), and MCPF, with different basis sets. Four different coordination modes of NO_2 to the metal have been considered. The C_{2v} η^2-O,O coordination mode is the most stable one for all metals. However, for $BeNO_2$ the ground state is a $^2B_1$ state while for the other metals the $^2A_1$ state is the most stable one. Our best estimates for the D_0 binding energies are 77 kcal mol^{-1} for $BeNO_2$, 53 kcal mol^{-1} for $MgNO_2$, 69 kcal mol^{-1} for $CaNO_2$, and 71 kcal mol^{-1} for $SrNO_2$.

Introduction

The study of the bonding in metal−ligand systems is a very active area of research,[1] owing to their applications in many fields, such as homogeneous and heterogeneous catalysis, environmental chemistry or biochemistry. In particular, the study of alkaline-earth metals interacting with different kind of ligands has been the subject of many studies.[2−11] Nitrogen oxides are unwanted pollutants that take part in important chemical reactions in the atmosphere. Because metal−NO_2 systems are known to be involved in the decomposition of nitrogen oxides, the study of the coordination of NO_2 to metals is important for understanding these processes.

Experimental studies of alkali[12−16] and alkaline-earth[17−20] metals with NO_2 suggest the existence of a long-lived $M^+NO_2^-$ complex. For alkali metals, the IR data are consistent with a planar ring structure of C_{2v} symmetry with an η^2-O,O bidentate coordination.[15,16] The IR data for the alkaline-earth metal nitrites suggest a similar structure or a nonplanar one with a poorly defined position of the metal lying above NO_2.[18]

From a theoretical point of view, few calculations have been reported for MNO_2 systems.[16,21−24] In agreement with the experimental results, the calculations for alkali metals show that the C_{2v} cyclic and the C_s *trans*-ONO structures are energy minima, the C_{2v} being the most stable one. For the transition metal systems Cu−NO_2 and Ag−NO_2, the C_{2v} η^2-O,O coordination mode was also found to be the ground-state structure.[24] Calculations on $[MNO_2]^+H_2O$ systems for alkaline-earth metals[25] have also recently been reported. To our knowledge no theoretical study has been performed for the neutral alkaline-earth−NO_2 complexes.

In this work we study the bonding in the MNO_2 systems for M = Be, Mg, Ca, and Sr. Calculations are done using both conventional ab initio methods and the density functional approach. One of the goals of the present work is to determine the ground-state structures and the vibrational frequencies for these systems. For this purpose we have studied four different coordination modes: the bidentate C_{2v} η^2-O,O and C_s η^2-N,O and the monodentate C_{2v} η^1-N and η^1-O modes. The nature of the different bonding mechanisms and the relative stabilities of the different isomers are analyzed as well as the trends in the group. Another important goal of these studies is to provide accurate binding energies for the alkaline-earth metal nitrites.

Computational Details

Molecular geometries and harmonic vibrational frequencies have been determined using the density functional approach. In these calculations we have used the hybrid Becke's three-parameter exchange functional[26] with the correlation functional of Lee, Yang, and Parr[27] (B3LYP). This functional has proved to provide reliable geometries and harmonic vibrational frequencies compared to more computational demanding ab initio correlated methods.[28−30] However, to confirm the reliability of the B3LYP binding energies, we have also done single-point calculations at the coupled cluster level with single and double excitations with a perturbative estimate of the triple excitations (CCSD(T))[31] at the B3LYP equilibrium geometries. In the calculations at the CCSD(T) level we have correlated all the electrons of Be and 10 electrons for Mg, Ca, and Sr. For N,O we have correlated the 2s and 2p electrons.

The same basis set has been used in these two levels of calculation. The N and O basis set is the (9s 5p)/[4s 2p] set developed by Dunning,[32] supplemented with a valence diffuse function (α_{sp} = 0.0639 for nitrogen and α_{sp} = 0.0845 for oxygen) and one d polarization function (α = 0.80 for nitrogen and α = 0.85 for oxygen). This basis set is referred to as D95+* in the Gaussian 94[33] program. The Be basis set is the (11s 5p)/[4s 3p] set given by Krishnan et al.[34] supplemented with a valence diffuse function (α_{sp} = 0.0207) and one d polarization function (α = 0.255). The Mg basis set is the (12s 9p)/[6s 5p] set of McLean and Chandler[35] supplemented with a d polarization function (α = 0.28). The Ca basis sets is the (12s 6p)/[8s 4p] set given by Roos, Veillard, and Vinot[36] supplemented with two diffuse p functions (0.09913 and 0.03464) and five d functions contracted (311) to three functions.[37] For Sr we have used the relativistic effective core potential (RECP) of Hay and Wadt[38] in which the 4s, 4p, and 5s orbitals are included in the valence space. We have used their (5s 6p) valence basis set. With use of a general contraction, the inner three s functions are contracted to two functions, the outermost two s functions are uncontracted, and the six p functions are contracted (321). Five d functions contracted (311) to three functions have been added.[7] The final basis sets are

[⊗] Abstract published in *Advance ACS Abstracts,* December 15, 1997.

S1089-5639(97)02418-3 CCC: $15.00
Published on Web 01/15/1998

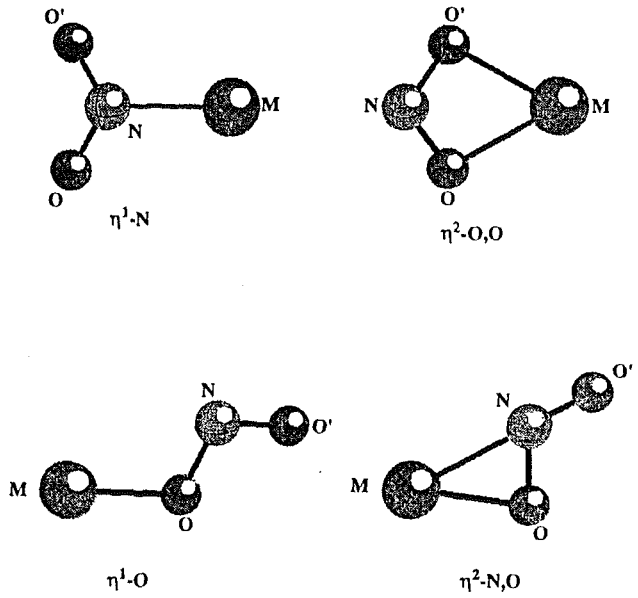

Figure 1. Studied coordination modes of NO_2 to the metal.

of the form (10s 6p 1d)/[5s 3p 1d] for N and O, (12s 6p 1d)/[5s 4p 1d] for Be, (12s 9p 1d)/[6s 5p 1d] for Mg, (12s 8p 5d)/[8s 6p 3d] for Ca, and (5s 6p 5d)/[4s 3p 3d] for Sr.

Single-point calculations using a larger atomic natural orbital (ANO) basis set have been carried out for the most stable isomer of each compound. These calculations have been performed using the modified coupled pair functional (MCPF)[39] method. The same electrons as in the CCSD(T) calculations have been correlated. For N and O we have used the (10s 5p 2d 1f)/[4s 3p 2d 1f] basis set of Dunning augmented with one diffuse s and one diffuse p functions.[40] This basis set, augmented with one diffuse d and one diffuse f functions, is referred to as aug-cc-pVTZ in the Gaussian 94 program.[33] For Be and Mg we have used the (14s 9p 4d 3f)/[5s 4p 3d 2f] and the (17s 12p 5d 4f)/[6s 5p 4d 3f] ANO basis sets of Widmark et al.,[41] respectively. For Ca and Sr we have used the (20s 15p 8d 6f)/[8s 7p 5d 3f] and (26s 19p 14d 4f)/[10s 10p 7d 3f] ANO basis set described in detail in reference 9.

The B3LYP and CCSD(T) calculations were performed using the Gaussian 94 program,[33] and open shell calculations were based on a spin-unrestricted treatment. The MCPF all-electron calculations were performed using the MOLCAS program,[42] while those calculations with Sr using pseudopotentials were performed using the SWEDEN-MOLECULE program.[43] In the MCPF case, the open shell calculations were based on a spin-restricted formalism.

Results and Discussion

Figure 1 shows the four different coordination modes of NO_2 to the metal that we have studied. For the η^2-O,O structures we have considered two different electronic states, the $^2A_1$ and the $^2B_1$ states. For the other coordinations we have only considered the ground state, that is, the $^2A_1$ state for the C_{2v} structures and the $^2A'$ for the C_s structures. The B3LYP optimal geometries and the B3LYP and CCSD(T) relative energies for the MNO_2 complexes are shown in Tables 1 and 2, respectively.

Table 2 shows that in all cases the most stable coordination mode is the η^2-O,O one. For $BeNO_2$ the ground state is the $^2B_1$ state, while for the other metals the $^2A_1$ state is the most stable one. The computed B3LYP relative energies are in quite good agreement with the CCSD(T) values, the only exception being the $^2B_1$ state for all metals due to the different nature of the bonding (see below). The ordering of stabilities between the different isomers is the same for Mg, Ca, and Sr, while for Be the η^1-O structure is more stable than the η^2-N,O one.

TABLE 1: B3LYP Optimal Geometries[a]

η^1-N Coordination ($^2A_1$)

	M–N	N–O	N–O'	MNO	ONO'
Be	1.634	1.246	1.246	118.0	124.1
Mg	2.085	1.247	1.247	118.7	122.5
Ca	2.273	1.252	1.252	119.0	122.1
Sr	2.427	1.253	1.253	119.1	121.7

η^1-O Coordination ($^2A'$)

	M–O	N–O	N–O'	MON	ONO'
Be	1.449	1.434	1.182	125.5	111.6
Mg	1.840	1.351	1.206	171.1	113.6
Ca	2.035	1.351	1.210	179.0	113.6
Sr	2.193	1.347	1.211	168.0	113.9

η^2-O,O Coordination ($^2A_1$)

	M–O	N–O	N–O'	OMO	ONO'
Be	1.680	1.283	1.283	76.3	107.9
Mg	2.089	1.275	1.275	61.1	112.7
Ca	2.311	1.278	1.278	54.9	112.9
Sr	2.477	1.277	1.277	51.0	113.2

η^2-O,O Coordination ($^2B_1$)

	M–O	N–O	N–O'	OMO	ONO'
Be	1.463	1.436	1.436	100.4	103.0
Mg	1.882	1.376	1.376	74.2	111.3
Ca	2.044	1.407	1.407	68.2	109.0
Sr	2.195	1.399	1.399	62.5	109.0

η^2-N,O Coordination ($^2A'$)

	M–O	M–N	N–O	N–O'	MON	ONO'	N–O	ONO
Be	1.529	1.800	1.361	1.196	76.8	118.6		
Mg	1.974	2.177	1.330	1.210	79.8	117.9		
Ca	2.192	2.365	1.317	1.215	80.5	118.7		
Sr	2.361	2.530	1.313	1.218	81.7	118.4		
NO_2 ($^2A_1$)							1.208	133.7
NO_2^- ($^1A_1$)							1.270	116.4
NO_2^{2-} ($^2B_1$)							1.380	113.7

[a] Bond lengths are in angstroms and bond angles in degrees.

The bonding mechanism between an alkaline-earth metal and NO_2 is believed to be initiated by long-range electron transfer from the metal to the NO_2 ligand, which leads to a charge-transfer $M^+NO_2^-$ complex.[17,19] Our calculations show an important ionic character for the MNO_2 complexes studied. In all cases except the $^2B_1$ state of the η^2-O,O structure, the last doubly occupied orbital of the complex is mainly the $6a_1$ orbital of NO_2. This orbital, which is schematically represented in Figure 2, is the single occupied orbital in the $^2A_1$ ground state of NO_2. The open shell orbital of the complex mainly corresponds to the s orbital of the metal. This orbital polarizes away from the ligand to reduce repulsion. This polarization takes place through sp hybridization for Be and Mg and through spd hybridization for Ca and Sr. The nature of these molecular orbitals is consistent with a bond with an important ionic $M^+NO_2^-$ character. Mulliken population analysis indicates that there is also some back-donation from the occupied orbitals of the ligand to the empty p and d orbitals of the metal. This back-donation is more important for Be complexes than for the other metal complexes studied. This view of the bonding is supported by the geometrical parameters shown in Table 1. The geometry of the NO_2 fragment in the η^2-O,O coordination ($^2A_1$ state) is in all cases very similar to that obtained for free NO_2^-. In the η^1-N coordination the geometrical parameters of the ligand are between those obtained for free NO_2^- and NO_2,

TABLE 2: Relative Energies of MNO_2 Complexes Computed at Several Levels of Calculation[a]

	Be		Mg		Ca		Sr	
structure	B3LYP	CCSD(T)	B3LYP	CCSD(T)	B3LYP	CCSD(T)	B3LYP	CCSD(T)
η^1-N	25.6	28.5	22.6	26.2	20.8	24.2	18.8	21.2
η^1-O	1.9	3.2	13.9	15.0	8.8	11.6	8.5	8.8
η^2-O,O($^2A_1$)	0.0	0.0	0.0	0.0	0.0	0.0	0.0	0.0
η^2-O,O($^2B_1$)	−13.7	−7.8	24.9	31.4	7.3	22.4	11.4	22.2
η^2-N,O	6.5	8.2	10.8	11.8	6.2	8.9	6.1	7.2

[a] Relative to the $^2A_1$ state of the η^2-O,O structure. In kcal mol^{-1}.

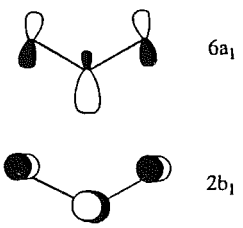

Figure 2. Schematic representation of the monooccupied $6a_1$ and first virtual $2b_1$ orbitals of NO_2.

indicating that for this coordination the covalent interaction between the metal and the ligand is larger than in the bidentate η^2-O,O structure. In the C_s structures the interpretation of the geometrical parameters is more difficult because the symmetry between the two NO bonds has been broken. However, it can be observed that the ONO angle is much closer to NO_2^- than to NO_2.

The ionic interaction is maximized in the η^2-O,O coordination mode by the approach of the metal atom along the C_{2v} axis between the two oxygen atoms. Thus, this coordination is the most stable one. The second most favorable ionic interaction takes place in the η^1-O structure. For the η^2-N,O structure the ionic stabilization is somewhat less favorable owing to the M−N interaction, and for the η^1-N isomer the ionic interaction is very inefficient. This is the order observed for Be complexes, since the differences between the ionic interactions are more important when the metal−ligand distances are smaller. However, in the case of Mg, Ca, and Sr, the η^2-N,O structure is slightly more stable than the η^1-O one. In these cases the more favorable overlap between the $6a_1$ orbital of NO_2 (see Figure 2) and the orbitals of the metal determines the order of stability of the η^1-O and η^2-N,O isomers.

The bonding mechanism corresponding to the $^2B_1$ state of the η^2-O,O coordination is different. The Mulliken population analysis shows that the charge over the metal is always larger than in the $^2A_1$ state. In this complex the last doubly occupied molecular orbital is mainly the $6a_1$ orbital of free NO_2 (as in the $^2A_1$ state) but now the open shell corresponds to an orbital that is mainly the $2b_1$ orbital of NO_2 (see Figure 2). This $2b_1$ orbital would be the first virtual orbital in free NO_2. Consistent with this, the Mulliken population analysis shows that in the $^2B_1$ state the unpaired electron is completely located in the NO_2 fragment of the complex. The nature of these orbitals shows that in the $^2B_1$ state there is some ionic $M^{2+}NO_2^{2-}$ contribution to the bonding. As in the case of the $^2A_1$ state, in addition to the electron-transfer mechanism there is also important back-donation from the occupied orbitals of NO_2 to the empty p and d orbitals of the metal atom. It can be observed in Table 1 that the geometrical parameters of the NO_2 fragment in the $^2B_1$ state are now more similar to those obtained at the same level of calculation for NO_2^{2-}. The M−O distances are shorter than in the $^2A_1$ state because the s orbital of the metal is empty and the repulsion with the ligand is smaller. The N−O distances are larger because now the antibonding $2b_1$ orbital of NO_2 is occupied.

Table 2 shows that the energy difference between the $^2A_1$ and the $^2B_1$ states of the η^2-O,O coordination varies significantly with the level of calculation. It is observed that the $^2B_1$ state is more stabilized with respect to the $^2A_1$ one at the B3LYP level than at the CCSD(T) one, the largest difference being determined for Ca and Sr. The use of the larger basis set reduces the difference between B3LYP and CCSD(T) results. However, for Ca both methods still differ by 9.1 kcal mol^{-1}. Part of this error may arise from the fact that the s−d excitation in Ca^+ is underestimated at the B3LYP level compared to CCSD(T). Considering that the d population is larger in the $^2B_1$ state than in the $^2A_1$ one, it is not surprising that Ca and Sr, which have low-lying d orbitals, show the largest differences.

It has already been mentioned that for all the alkaline-earth metals considered the most stable structure corresponds to the η^2-O,O coordination. However, although for Be the ground state is the $^2B_1$ state, for the rest of the metals the $^2A_1$ state is the lowest one. The Be atom has the smallest atomic radius; its inner electron shell contains only the 1s electrons, and so the closed shell repulsion with the ligand is smaller than in the rest of the alkaline-earth metals considered. This fact allows Be to get closer to the ligand, and thus, the stabilizing interactions are stronger for the Be complexes. Therefore, in the case of Be the $^2B_1$ state becomes more stable than the $^2A_1$ state because these strong interactions compensate the cost of transferring a second electron to the ligand. This is not the case with the other alkaline-earth metals studied, where the metal−ligand distances are larger than for Be complexes. For the other coordination modes of the $BeNO_2$ complex, the electronic state equivalent to the $^2A_1$ state is always more stable than the one involving the occupation of the $2b_1$ orbital of NO_2.

The harmonic vibrational frequencies computed for the most stable electronic state of each coordination are presented in Table 3. All coordination modes have been found to be minima on the potential energy surface except the η^1-N structure for all metals and the η^1-O isomer of $MgNO_2$. The η^1-N structure is a transition state connecting two equivalent η^2-N,O minima. For $MgNO_2$, the η^1-O transition state connects the η^2-O,O and the η^2-N,O minima. It can be observed in Table 3 that the first frequency of the η^1-O coordination, which corresponds to the bending of the MON angle, is very low for all metals except Be, indicating that the potential energy surface is very flat. Therefore, the only structures that one would expect to detect in experiments are the η^2-N,O and η^2-O,O structures.

Let us consider the largest three frequencies of each case that correspond to the vibrations of the NO_2 fragment. If one compares the frequencies associated with the NO_2 fragment of the same coordination mode but for the different metals, it can be observed that they are always very similar, especially for Mg, Ca, and Sr compounds. This indicates that the nature of the NO_2 fragment remains more or less the same regardless of

TABLE 3: Harmonic Vibrational Frequencies[a] Computed at B3LYP Level

η^1-N Coordination

	M−NO_2 in-plane wag (b_2)	M−NO_2 out-of-plane wag (b_1)	M−NO_2 stretch (a_1)	NO_2 bend (a_1)	NO stretch (b_2)	NO stretch (a_1)
Be ($^2A_1$)	190*i*	403	621	896	1516	1438
Mg ($^2A_1$)	116*i*	311	344	790	1486	1368
Ca ($^2A_1$)	180*i*	214	288	790	1462	1406
Sr ($^2A_1$)	165*i*	173	231	784	1452	1401

η^1-O Coordination

	M−NO_2 in-plane wag (a′)	M−NO_2 out-of-plane wag (a″)	M−NO_2 stretch (a′)	NO_2 bend (a′)	NO stretch (a′)	NO stretch (a′)
Be ($^2A'$)	186	125	579	828	1136	1746
Mg ($^2A'$)	87*i*	39	447	813	1035	1620
Ca ($^2A'$)	83	62	386	801	1006	1612
Sr ($^2A'$)	35	57	298	793	1018	1603

η^2-O,O Coordination

	M−NO_2 in-plane wag (b_2)	M−NO_2 out-of-plane wag (b_1)	M−NO_2 stretch (a_1)	NO_2 bend (a_1)	NO stretch (b_2)	NO stretch (a_1)
Be ($^2B_1$)	581	333	633	965	1174	1121
Mg ($^2A_1$)	293	217	388	864	1285	1333
Ca ($^2A_1$)	243	149	314	823	1249	1339
Sr ($^2A_1$)	219	143	253	821	1257	1341

η^2-N,O Coordination

	M−NO_2 in-plane wag (a′)	M−NO_2 out-of-plane wag (a″)	M−NO_2 stretch (a′)	NO_2 bend (a′)	NO stretch (a′)	NO stretch (a′)	NO_2 bend (a_1)	NO stretch (b_2)	NO stretch (a_1)
Be ($^2A'$)	122	295	726	839	1102	1701			
Mg ($^2A'$)	169	236	480	766	1109	1630			
Ca ($^2A'$)	189	238	394	775	1135	1609			
Sr ($^2A'$)	167	225	319	775	1151	1589			
NO_2 ($^2A_1$)							741	1701	1387
NO_2^- ($^1A_1$)							780	1321	1338
NO_2^{2-} ($^2B_1$)							584	868	1004

[a] In cm^{-1}.

the metal considered. It can also be observed that for the η^2-O,O coordination in the $^2A_1$ state (Mg, Ca, and Sr) the frequencies resemble more those of free NO_2^- than those of free NO_2 or NO_2^{2-}, confirming again the $M^+NO_2^-$ character in these complexes. In the $^2B_1$ state of the η^2-O,O coordination of $BeNO_2$ the values of the two NO stretchings are smaller than in the rest of the η^2-O,O structures, approaching the values of NO_2^{2-}.

In the η^1-N coordination mode the two NO stretching values are always larger than in the η^2-O,O isomers, proving the larger covalent contribution to the bond in this coordination. Moreover, the relative ordering values in this coordination between the two NO stretchings are the same as in NO_2 and the opposite in NO_2^-. In the C_s structures, η^2-N,O and η^1-O, the values of the two NO stretching frequencies are very different. This is due to the fact that in this coordination the C_{2v} symmetry has been lost with a lengthening of the NO bond interacting with the metal and a shortening of the terminal NO bond compared to free NO_2^-.

Tevault and Andrews[18] reported an experimental value of 1244 cm^{-1} for the frequency corresponding to the asymmetric stretching of the NO_2 fragment in the $CaNO_2$ and $SrNO_2$ complexes in rare-gas matrixes and another value of 1223 cm^{-1} only for $SrNO_2$ complex. They suggested a nonplanar structure of the complex with a poorly defined position of M^+ above the plane of the ligand associated with the first value and a coplanar structure associated with the second one. All our attempts to calculate a nonplanar η^2-O,O structure collapsed to the planar one. In any case, both experimental values are in very good agreement with the values computed for the NO asymmetric stretching of $CaNO_2$ and $SrNO_2$ (1249 and 1257 cm^{-1}, respectively).

TABLE 4: D_e Binding Energies for the Ground States of the MNO_2 Complexes[a]

	Be	Mg	Ca	Sr
B3LYP[b]	80.8	47.2	70.1	67.9
CCSD[b]	70.2	50.4	68.1	71.3
CCSD(T)[b]	68.7	48.9	66.0	69.3
MCPF[b]	69.8	49.8	67.1	70.6
MCPF[c,d]	78.8 (77.2)	53.4 (52.6)	69.1 (68.7)	71.4 (71.1)

[a] In kcal mol^{-1}. [b] Smaller basis set. [c] Larger basis set. [d] In parentheses are shown the D_0 binding energies computed using the B3LYP harmonic frequencies.

Table 4 presents the bond dissociation energies, with respect to neutral M and NO_2, of the ground-state structure of each complex. These binding energies are computed at different levels of calculation and using different basis sets. By comparing the B3LYP values with the CCSD(T) ones, one can observe that for Mg, Ca, and Sr the computed binding energies are very similar while for $BeNO_2$ the difference is 12.1 kcal mol^{-1}.

The CCSD(T) calculations with the larger basis set were computationally too demanding, so we have done the calculations at the MCPF level, which provide results similar to those at CCSD and CCSD(T) levels with the smaller basis set (see Table 4). Thus, one can expect that with the larger basis set the MCPF and CCSD(T) values will also be similar. MCPF values show that the computed binding energy increases with the size of the basis set. For Mg, Ca, and Sr the differences are small, while in the case of Be the difference is more important (9.0 kcal mol^{-1}). It seems that at the CCSD(T) and MCPF levels with the smaller basis set, the binding energy of $BeNO_2$ is underestimated. The B3LYP dissociation energy is less sensitive to the basis set. The value computed with the larger basis set for $BeNO_2$ is 77.0 kcal mol^{-1}.

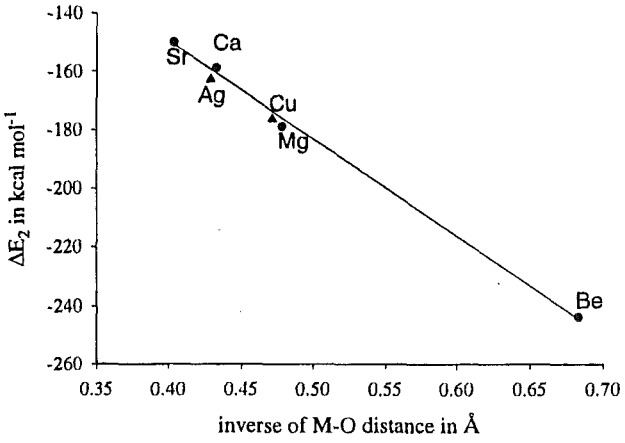

Figure 3. Energy of formation of MNO_2 relative to the ions (ΔE_2) plotted against the reciprocal of the M−O bond distance for the ground-state structure of each complex. The values corresponding to $CuNO_2$ and $AgNO_2$, taken from reference 24, are included for comparison.

In all cases, the MCPF binding energies computed with the larger basis set are in good agreement with the initial values obtained at the B3LYP level with the smaller basis set; the main difference can be observed in the case of the Mg complex (6.2 kcal mol^{-1}). Therefore, one can conclude that for these alkaline-earth metal complexes the values of the binding energies computed at the B3LYP level with a relatively small basis set seem to be good enough when compared with those values computed at the MCPF level using a large basis set.

Let us now consider the variation of the binding energy when changing the metal. The Be complex presents the strongest bond, while the binding energies corresponding to Mg, Ca, and Sr complexes increase when going down in the group. The values computed for Ca and Sr are very similar, while for Mg the binding energy is notably smaller. The binding energy of a complex with an important ionic nature can be formally decomposed into two contributions. The first one, ΔE_1, would involve the formation of the M^+ and NO_2^- ions from the neutral fragments. The second contribution, ΔE_2, would correspond to the interaction between both ions.

$$D_e = -(\Delta E_1 + \Delta E_2)$$

ΔE_1 includes the first ionization potential of the metal atom and the adiabatic electron affinity of NO_2. This second term remains constant along the group so that the variation of ΔE_1 is determined by the ionization potential of the metal. ΔE_2 is the formation energy of MNO_2 relative to the M^+ and NO_2^- ions. Figure 3 represents the variation of ΔE_2 with respect to the inverse of the M−O bond distance for the studied complexes. The observed linear variation corresponds to what is expected for complexes with an important ionic nature.[44,45] The variation of D_e for Mg, Ca, and Sr complexes is determined by the variation of the ionization potential of the metal (the computed MCPF values are 7.58 eV for Mg, 6.03 eV for Ca, and 5.55 eV for Sr). On the other hand, the difference between the values of D_e corresponding to Mg and Be is governed by the ΔE_2 term. ΔE_2 is extremely stabilizing in $BeNO_2$ owing to the small size of Be. This allows Be to have the largest binding energy despite its large ionization potential (the computed MCPF value is 9.29 eV). It can also be observed in Figure 3 that, although Cu and Ag are transition metals, the nature of the bonding in $CuNO_2$ and $AgNO_2$[24,46] is analogous to that found in the alkaline-earth nitrite complexes.

Conclusions

The structure, binding energies, and vibrational frequencies of different coordination modes have been determined for the MNO_2 system (M = Be, Mg, Ca, Sr). The η^2-O,O coordination is the most stable one for all the metals studied, as was previously found for the alkali and the Cu and Ag nitrite complexes. In the case of Mg, Ca, and Sr, the ground state is a $^2A_1$ state while for Be it is a $^2B_1$ state. This $^2B_1$ state presents a different bonding mechanism, and it is geometrically very different from the $^2A_1$ state. The B3LYP values for the binding energy obtained with a double-ζ plus polarization quality basis set are very similar to those obtained at the MCPF level with a large ANO basis set. Our best calculation for the D_0 binding energies are 77 kcal mol^{-1} for $BeNO_2$, 53 kcal mol^{-1} for $MgNO_2$, 69 kcal mol^{-1} for $CaNO_2$, and 71 kcal mol^{-1} for $SrNO_2$. The variation of the binding energies agrees with a metal−ligand bond of basically ionic character.

Acknowledgment. This work has been financially supported by DGICYT (PB95-0640) and CIRIT (SGR95-00401). Computer time from the Centre de Supercomputació de Catalunya (CESCA) is gratefully acknowledged. L.R. gratefully acknowledges the Spanish Ministry of Education and Science for a doctoral fellowship.

References and Notes

(1) See, for example, the following. (a) Veillard, A. *Chem. Rev.* **1991**, *91*, 743. (b) *Organometallic Ion Chemistry*; Freiser, B. S., Ed.; Kluwer Academic Publishers: Dordrecht, 1996.
(2) Partridge, H.; Bauschlicher, C. W.; Langhoff, S. R. *Chem. Phys. Lett.* **1984**, *109*, 446.
(3) Langhoff, S. R.; Bauschlicher, C. W.; Partridge, H.; Ahlrichs, R *J. Chem. Phys.* **1986**, *84*, 5025.
(4) Balaji, V.; Jordan, K. D. *J. Phys. Chem.* **1988**, *92*, 3101.
(5) Seijo, L.; Barandiarán, Z.; Huzinaga, S. *J. Chem. Phys.* **1991**, *94*, 3762.
(6) Kaupp, M.; Schleyer, P. v. R.; Stoll, H.; Preuss, H. *J. Am. Chem. Soc.* **1991**, *113*, 6012.
(7) Bauschlicher, C. W.; Sodupe, M.; Partridge, H. *J. Phys. Chem.* **1992**, *96*, 4453.
(8) Kaupp, M.; Schleyer, P. v. R. *J. Phys. Chem.* **1992**, *96*, 7316.
(9) Bauschlicher, C. W.; Partridge, H.; Sodupe, M.; Langhoff, S. R. *J. Phys. Chem.* **1992**, *96*, 9259.
(10) Hanusa, T. P. *Chem. Rev.* **1993**, *93*, 1023.
(11) Bauschlicher, C. W.; Langhoff, S. R; Partridge, H. *J. Chem. Phys.* **1994**, *101*, 2644.
(12) Herm, R. R.; Herschbach, D. R. *J. Chem. Phys.* **1970**, *52*, 5783.
(13) Ham, D. O.; Kinsey, J. L. *J. Chem. Phys.* **1970**, *53*, 285.
(14) Milligan, D. E.; Jacox, M. E. *J. Chem. Phys.* **1971**, *55*, 3404.
(15) Barbeschi, M.; Bencivenni, L.; Ramondo, F. *Chem. Phys.* **1987**, *112*, 387.
(16) Lo, W. J.; Shen, M. Y.; Yu, C. H.; Lee, Y. P. *J. Chem. Phys.* **1996**, *104*, 935.
(17) Herm, R. R.; Lin, S. M.; Mims, C. A. *J. Phys. Chem.* **1973**, *77*, 2931.
(18) Tevault, E.; Andrews, L. *Chem. Phys. Lett.* **1977**, *48*, 103.
(19) Davis, H. F.; Suits, A. G.; Lee, Y. T. *J. Chem. Phys.* **1992**, *96*, 6710.
(20) Cheong, B. S.; Parson, J. M. *J. Chem. Phys.* **1994**, *100*, 2637.
(21) Goddard, J. D.; Klein, M. L. *Phys. Rev. A* **1983**, *28*, 1141.
(22) Ramondo, F. *Chem. Phys. Lett.* **1989**, *156*, 346.
(23) Ramondo, F.; Bencivenni, L.; Sanna, N.; Nunziante Cesaro, S. *J. Mol. Struct.: THEOCHEM* **1992**, *253*, 121.
(24) Rodríguez-Santiago, L.; Branchadell, V.; Sodupe, M. *J. Chem. Phys.* **1995**, *103*, 9738.
(25) Rossi, V.; Sadun, C.; Bencivenni, L.; Caminiti, R. *J. Mol. Struct.: THEOCHEM* **1994**, *314*, 247.
(26) Becke, A. D. *J. Chem. Phys.* **1993**, *98*, 5648.
(27) Lee, C.; Yang, W.; Parr, R. G. *Phys. Rev. B* **1988**, *37*, 785.
(28) Holthausen, M. C.; Heineman, C.; Cornehl, H. H.; Koch, W.; Schwarz, H. *J. Chem. Phys.* **1995**, *102*, 4931.
(29) Rodríguez-Santiago, L.; Sodupe, M.; Branchadell, V. *J. Chem. Phys.* **1996**, *105*, 9966.

(30) Bauschlicher, C. W.; Ricca, A.; Partridge, H.; Langhoff, S. R. in *Recent Advances in Density Functional Theory*; Chong, D. P., Ed.; World Scientific Publishing Company: Singapore, 1997; Part II.

(31) Raghavachari, K.; Trucks, G. W.; Pople, J. A.; Head-Gordon, M. *Chem. Phys. Lett.* **1989**, *57*, 479.

(32) Dunning, T. H. *J. Chem. Phys.* **1970**, *53*, 2823.

(33) Frisch, M. J.; Trucks, G. W.; Schlegel, H. B.; Gill, P. M. W.; Johnson, B. G.; Robb, M. A.; Cheesman, J. R.; Keith, T. A.; Petersson, G. A.; Montgomery, J. A.; Raghavachari, K.; Al-Laham, M. A.; Zakrzewsky, V. G.; Ortiz, J. V.; Foresman, J. B.; Cioslowsky, J.; Stefanov, B.; Nanayakkara, A.; Challacombe, M.; Peng, C. Y.; Ayala, P. Y.; Chen, W.; Wong, M. W.; Andrés, J. L.; Replogle, E. S.; Gomperts, R.; Martin, R. L.; Fox, D. J.; Binkley, J. S.; Defrees, D. J.; Baker, J.; Stewart, J. J. P.; Head-Gordon, M.; Gonzalez, C.; Pople, J. A. *Gaussian 94*, Revision D.1; Gaussian Inc.: Pittsburgh, PA, 1995.

(34) Krishnan, R.; Binkley, J. S.; Seeger, R.; Pople, J. A. *J. Chem. Phys.* **1980**, *72*, 650.

(35) McLean, A. D.; Chandler, G. S. *J. Chem. Phys.* **1980**, *72*, 5639.

(36) Roos, B.; Veillard, A.; Vinot, G. *Theor. Chim. Acta* **1971**, *20*, 1.

(37) Petterson, L. G.; Siegbahn, P. E. M.; Ismaail, S. *Chem. Phys.* **1983**, *82*, 355.

(38) Hay, P. J.; Wadt, W. R. *J. Chem. Phys.* **1985**, *82*, 299.

(39) Chong, D. P.; Langhoff, S. R. *J. Chem. Phys.* **1986**, *84*, 5606. Alrichs, R.; Scharf, P.; Ehrhardt, C. *J. Chem. Phys.* **1984**, *82*, 890.

(40) Kendall, R. A.; Dunning, T. H. *J. Chem. Phys.* **1992**, *96*, 6796.

(41) (a) Widmark, P. O.; Malmqvist, P. A.; Roos, B. O. *Theor. Chim. Acta* **1990**, *77*, 201. (b) Widmark, P. O.; Persson, B. J.; Roos, B. O. *Theor. Chim. Acta* **1991**, *79*, 419.

(42) Anderson, K.; Blomberg, M. R. A.; Fülscher, M. P.; Kellö, V.; Lindh, R.; Malmqvist, P. Å.; Noga, J.; Olsen, J.; Roos, B. O.; Sadlej, A. J.; Siegbahn, P. E. M.; Urban, M.; Widmark, P. O. *MOLCAS*, Version 3; University of Lund: Sweden, 1994.

(43) SWEDEN-MOLECULE is an electronic structure program written by the following: Almlöf, J.; Bauschlicher, C. W.; Blomberg, M. R. A.; Chong, D. P.; Heiberg, A.; Langhoff, S. R.; Malmqvist, P. Å.; Rendell, A. P.; Siegbahn, P. E. M.; Taylor, P. R.

(44) Langhoff, S. R.; Bauschlicher, C. W.; Partridge, H. *J. Chem. Phys.* **1986**, *84*, 1687.

(45) Partridge, H.; Bauschlicher, C. W.; Sodupe, M.; Langhoff, S. R. *Chem. Phys. Lett.* **1992**, *195*, 200.

(46) Worden, D.; Ball, D. W. *J. Phys. Chem.* **1992**, *96*, 7167.

6. "Coordination of NO_2 to Cu and Mg in $M(NO_2)_2$ Complexes. A Theoretical Study"

Coordination of NO_2 to Cu and Mg in $M(NO_2)_2$ Complexes. A Theoretical Study[1]

Luis Rodríguez-Santiago, Xavier Solans-Monfort, Mariona Sodupe*, Vicenç Branchadell*

Departament de Química, Universitat Autònoma de Barcelona, Edifici Cn, 08193 Bellaterra, Spain.

Abstract

The geometries, vibrational frequencies and metal-ligand bond dissociation energies of 18 different structures of the $Cu(NO_2)_2$ complex have been studied. $Mg(NO_2)_2$ and $Cu(NO_3)_2$ have also been studied for comparison. The most stable structure of $Cu(NO_2)_2$ and $Cu(NO_3)_2$ corresponds to a D_{2h} one with a coplanar η^2-O,O coordination for the two NO_2 ligands. For $Mg(NO_2)_2$ the most stable structure is a D_{2d} one. The bonding in the D_{2h} and D_{2d} structures of $Cu(NO_2)_2$ is analyzed. For the MNO_2 systems the binding energy is very similar with both metals, while for the $M(NO_2)_2$ complexes the difference when changing the metal is very important. This behavior is related to the first and second ionization potentials of Cu and Mg. The computed vibrational frequencies are in good agreement with the available experimental data.

[1]Enviado a *Inog. Chem.*

Introduction

Transition metal-ligand interactions have been the focus of great attention during the last years,[1] due to its great number of applications. These applications include many fields, such as biochemistry, environmental chemistry, development of new materials or catalysis. The determination of accurate binding energies and geometries[1a,2] of the metal-ligand systems are of great interest for the development of these applications. Computational chemistry methods have proved to be very efficient in obtaining binding energies and geometries. Moreover, the critical step in catalysis is often the breaking of the first bond of a small metal cluster, but in experimental studies the energy that is frequently determined is the average metal-ligand bond energy. So, it is important the understanding of how the bonding changes with the number of ligands.

Nitrite coordination complexes have been very studied from the earliest days of coordination chemistry due to this ability of NO_2 to coordinate to a metal in different ways.[3] Each type of NO_2 coordination leads to different properties of the compound. Furthermore, nitrogen oxides (NO_x x=1,2) are unwanted pollutants that take part in important chemical reactions in the atmosphere, and in corrosion. Thus, coordination of NO_2 to a metal as well as the interaction of successive NO_x ligands can provide important information for the understanding of these processes. The interaction of NO_2 with alkaline,[4-11] alkaline-earth[12-16] and transition metals[17-20], have been studied by several authors both, theoretically and experimentally.

Theoretical calculations for $M(NO_3)_2$ with M=Be, Mg and Ca systems have been

performed by Rossi et al. at the HF level.[21] The results obtained for the $Mg(NO_3)_2$ system were used for the assignment of the FT-IR matrix isolation spectrum of the stable gas phase molecule $Cu(NO_3)_2$. From this assignment, they conclude that both NO_3 groups are equivalent and lie in the same plane, in agreement with earlier electron diffraction studies.[22] On the other hand, experimental IR matrix studies have been carried out on the $Cu(NO_2)_2$ system by Worden and Ball.[17] This system is very similar to $Cu(NO_3)_2$, and one would expect both molecules to have the same structure. However, the authors consider that the most probable structure for $Cu(NO_2)_2$ implies two different NO_2 groups.

In order to elucidate the structure of $Cu(NO_2)_2$, we have performed calculations using density functional and conventional ab initio methods. We have studied all the possible coordination modes of two NO_2 molecules to a Cu atom. The bonding mechanism of the most stable structure has been analyzed. We have also performed calculations on the $Cu(NO_3)_2$ and $Mg(NO_2)_2$ systems in order to compare them with the $Cu(NO_2)_2$ complex.

Computational details

Molecular geometries and harmonic vibrational frequencies have been determined using the density functional approach. In these calculations we have used the hybrid Becke's three parameter exchange functional[23] with the correlation functional of Lee Yang and Parr[24] (B3LYP). This method has proved to provide reliable geometries and harmonic vibrational frequencies compared to more computational demanding ab initio correlated methods.[2,25] However, in order to confirm the reliability of the B3LYP binding energies, we have also done single point calculations at the coupled cluster level with single and double excitations and a

perturbative estimate of the triple excitations[26] (CCSD(T)) at the B3LYP equilibrium geometries. In the calculations at the CCSD(T) level we have correlated the 3d and 4s electrons of Cu and the 2s, 2p and 3s electrons of Mg. For N and O we have correlated the 2s and 2p electrons.

The same basis set has been used in these two levels of calculation. The N and O basis set is the (9s 5p)/[4s 2p] set developed by Dunning,[27] supplemented with a valence diffuse function (α_{sp}=0.0639 for nitrogen and α_{sp}=0.0845 for oxygen) and one d polarization function (α=0.80 for nitrogen and α=0.85 for oxygen). This basis set is referred to as D95+* in the GAUSSIAN-94 program.[28] The Cu basis set is a [8s 4p 3d] contraction of the (14s 9p 5d) primitive set of Wachter[29] supplemented with two diffuse p and one diffuse d function.[30] The Mg basis set is the (12s 9p)/[6s 5p] set of McLean and Chandler[31] supplemented with a d polarization function (α=0.28). The final basis sets are of the form (10s 6p 1d)/[5s 3p 1d] for N and O, (14s 11p 6d)/[8s 6p 4d] for Cu and (12s 9p 1d)/[6s 5p 1d] for Mg.

Single-point CCSD(T) calculations using a larger basis set have also been carried out for the most stable structure of each complex. In these calculations the Cu basis set is further augmented by a single contracted set of f polarization functions that is based on a three-term fit to a Slater-type orbital, which leads to a (14s 11p 6d 3f)/[8s 6p 4d 1f] basis set.[32] For Mg we have used the (16s 12p 3d 2f)/[6s 5p 3d 2f] basis set of Dunning referred as cc-pVQZ in MOLPRO 96 program.[33] For N and O we have used the (10s 5p 2d 1f)/[4s 3p 2d 1f] basis set of Dunning augmented with one diffuse s and one diffuse p functions[34]. This basis set, augmented with one diffuse d and one diffuse f functions, is referred to as aug-cc-pVTZ.

The B3LYP calculations were performed using the GAUSSIAN-94[28] program and open shell calculations were based on a spin unrestricted treatment, while the CCSD(T) results were performed with the MOLPRO[33] program and were based on a spin restricted formalism.

Results and discussion

Figure 1 shows the four different coordination modes of NO_2 to a metal atom considered in our study. NO_2 can act both as a monodentate ligand or as a bidentate ligand when interacting with a metal atom. As a monodentate ligand, NO_2 can interact with the metal through the oxygen (η^1-O) or through the nitrogen (η^1-N). As a bidentate ligand, it can interact with the two oxygens (η^2-O,O) or with one nitrogen-oxygen bond (η^2-N,O). In the present work we have investigated all the possible structures that can be obtained with two NO_2 molecules coordinated to a Cu atom combining the four coordination modes shown in Figure 1 and considering for each case two different orientations for the NO_2 ligands: coplanar and perpendicular.

Among all the possible structures, only 18 have been found as stationary points on the potential energy surface of the $Cu(NO_2)_2$ system. The B3LYP relative energies of these structures are shown in Table 1. Figure 2 shows the B3LYP geometrical results for the structures characterized as energy minima. It can be observed in Table 1 that the most stable structure has D_{2h} symmetry and corresponds to the two NO_2 ligands bonded to the Cu atom with the η^2-O,O coordination in the same plane (AA structure). The D_{2d} structure with the two NO_2 ligands acting with η^2-O,O coordination, in perpendicular planes (AAp structure) is 23.7 kcal mol^{-1} above the AA structure. In general, the most stable structures are those in which one

of the two NO_2 fragments acts with the η^2-O,O coordination. The less stable structures are, in general, those with one of the two NO_2 fragments coordinated through the N atom (η^1-N coordination).

The geometry parameters of the η^2-O,O moiety in all structures are very similar to those computed for free NO_2^- (r(NO)=1.270 Å and ∠ONO=116.4°). In the fragments with η^2-N,O and η^1-O coordination the symmetry between the two NO bonds of each NO_2 has been broken, however, we can see that the ONO angle in the η^1-O coordinations is close to the value of this angle in NO_2^-, while in the η^2-N,O coordinations the ONO angle lies within the values obtained for NO_2^- and NO_2 (∠ONO=133.7°). This shows that the bonding between the Cu atom and the two NO_2 molecules has an important ionic contribution. Thus, the most favorable structure for the ionic interaction is the AA structure where the metal atom interacts with the four oxygen atoms. The second most favorable ionic interaction takes place in the η^1-O coordination. The few exceptions to this general observation are due to the differences in the metal-ligand covalent interactions.

Let us now analyze the bonding in the $^2B_{3g}$ ground state of the most stable D_{2h} structure, AA, and in the $^2B_2$ state of the D_{2d} structure, AAp. Figure 3 shows a schematic orbital interaction diagram between Cu and two NO_2 molecules both for the D_{2h} and D_{2d} structures. The bonding in the D_{2h} structure can be described as the interaction of the $^2D(d^9)$ state of Cu^{2+} and the $(NO_2)_2^{2-}$ fragment. It can be observed in Figure 3 that the open shell in this structure arises from a three-electron interaction between the b_{3g} symmetry adapted combination of the $4b_2$ orbitals of the NO_2 molecules and the d_{yz} orbital of the metal. Moreover, there is a very important donation from the a_g combination of the $6a_1$ orbitals of NO_2 to the 4s metal orbital.

The bonding can also be viewed as the interaction of the ^3D (d^9s^1) state of Cu^+, where there is a 3d-4s promotion in the metal in order to reduce repulsion with the ligands, and the $(NO_2)_2^-$ fragment. The metal Mulliken population analysis shows a situation in between both descriptions. The metal population is $4s^{0.75}$ $3d^{9.39}$ and the unpaired electron is distributed 0.6 in the metal and 0.4 in the ligands. If we consider the $^2B_2$ state of the D_{2d} structure, it can be observed that the open shell arises from a three-electron interaction of the d_{xy} orbital of the metal and the b_2 combination of the $6a_1$ orbitals of NO_2, and that there is also an important donation from the ligands to the 4s orbital of Cu^{2+}.

The orbital of NO_2 that has the larger overlap with the metal is the $4b_2$ orbital. Thus the orbitals of the $(NO_2)_2$ fragment that interact more strongly with the metal atom are $4b_{3g}$ and $4b_{2u}$ in the D_{2h} structure, and 5e in the D_{2d} one. The energy difference between both structures mainly arises from the interaction of these orbitals with the metal. For the D_{2d} structure the 5e orbitals of the $(NO_2)_2$ fragments form two destabilizing four-electron interactions. On the other hand, in the D_{2h} structure the $4b_{3g}$ orbital forms one three electron interaction, and the $4b_{2u}$ orbital remains in the complex as a non bonding orbital. So, the D_{2d} structure is destabilized with respect to the D_{2h} one due to a larger repulsive metal-ligand interaction involving the 3d electrons of the metal.

The examination of the orbital interaction diagram of the D_{2d} $Cu(NO_2)_2$ complex shows that it is possible that the ground state is not the one considered but a ^2E state in which the open shell orbital would be one of the 7e orbitals while the $7b_2$ orbital would be doubly occupied. We have carried out the calculation of the ^2E state starting from the geometry of the $^2B_2$ state. At this geometry, the ^2E state is 1.5 kcal mol^{-1} higher in energy than the $^2B_2$ state.

Geometry relaxation reduce the D_{2d} symmetry to C_{2v}. The optimization leads to a structure corresponding to a $^2B_2$ state in C_{2v} symmetry that is 16 kcal mol^{-1} higher in energy that the global D_{2h} minimum. This C_{2v} structure has an imaginary frequency associated to a rotation that connects two equivalent D_{2h} minima. In any case, both if the ground state of the D_{2d} structure is a $^2B_2$ or a ^2E state, the discussion about the interactions of the $(NO_2)_2$ fragment with the metal based on the orbital interaction diagram presented in Figure 3 would be similar.

Let us now consider a system where the metal atom has no d occupied orbitals, such as the $Mg(NO_2)_2$ complex. Figure 4 shows the B3LYP optimized geometries for the D_{2h} and D_{2d} structures of the $Mg(NO_2)_2$ system. The computed values for the geometrical parameters are almost identical for both structures. In contrast to the $Cu(NO_2)_2$ system, for $Mg(NO_2)_2$ the D_{2d} structure is the global minimum, the D_{2h} structure being a transition state that connects two equivalent D_{2d} minima. The energy difference between both structures is only 2.5 kcal mol^{-1} at the B3LYP level. In the $Mg(NO_2)_2$ complex there are no occupied d orbitals on the metal and, therefore, the order of stability is determined by the steric repulsion between the ligands. This repulsion is slightly larger in the D_{2h} structure than in the D_{2d} one.

The only experimental data available for $Cu(NO_2)_2$ correspond to vibrational frequencies measured in Ar matrix by Worden and Ball.[17] These authors suggest that in the $Cu(NO_2)_2$ complex the two NO_2 ligands would be coordinated in different ways. On the other hand, the gas phase structure of $Cu(NO_3)_2$ determined from electron diffraction experiments[22] shows a D_{2h} structure in which the coordination mode of the two NO_3 ligands is the same. We have calculated the D_{2h} structure for the $Cu(NO_3)_2$ molecule and the obtained geometry is shown in Figure 5. We can see that the computed results are in very good agreement with the

gas phase experimental geometry of the $Cu(NO_3)_2$ molecule. The ground state of this molecule is a $^2B_{3g}$ state, as in $Cu(NO_2)_2$, and the bonding mechanism is the same in both cases. Thus, one can conclude that the most stable structure of the $Cu(NO_2)_2$ system should also have D_{2h} symmetry, with two equivalent NO_2 ligands, as determined by our calculations.

The harmonic vibrational frequencies computed for the ground state structure of $Cu(NO_2)_2$ and $Mg(NO_2)_2$ complexes are presented in Table 2. It can be observed that for both systems the values for the NO symmetric stretching are larger than the values for the NO asymmetric stretching, the difference between both frequencies being small. The same behavior is observed for free NO_2^-, while for NO_2 the ordering between both NO stretching frequencies is reversed and the difference between them is large. These facts confirm again that the NO_2 fragments of the complex have an important NO_2^- character.

Worden and Ball reported the infrared spectra of NO_2 reacting with vaporized Cu and condensed together in Ar matrices. Three frequencies were assigned to the $Cu(NO_2)_2$ system: 1214, 1192 and 1173 cm^{-1}. Three possible structures are considered: $Cu^{2+}(NO_2^-)_2$, $Cu^+(N_2O_4^-)$, and $Cu^+(NO_2^-)NO_2$, where both NO_2 molecules are not equivalent. The IR data do not allow to discriminate between them, but these authors consider the later as the most probable one. Thus, they assign the frequency of 1214 cm^{-1} to the asymmetric NO stretching of NO_2^-, while the other two frequencies are assigned to the same absorption but shifted due to structural isomerism of the NO_2 units or due to matrix effects. We have performed calculations on the $Cu^+(N_2O_4^-)$ system and the results show that all the possible structures lie higher in energy than the $Cu(NO_2)_2$ D_{2h} structure (between 36.8 kcal mol^{-1} and 50.9 kcal mol^{-1}, depending on the coordination) . On the other hand, the structures shown in Table 1 with both NO_2 molecules

coordinated in different ways lie also higher in energy. The same assignment made by Worden and Ball for the three observed frequencies would be valid for a $Cu^{2+}(NO_2^-)_2$ structure. So, our results in favor of a D_{2h} structure with two equivalent NO_2 ligands for the $Cu(NO_2)_2$ system can be compatible with the IR results reported by Worden and Ball. Our calculated value for the asymmetric NO stretching, 1254 cm^{-1}, is in excellent agreement with the experimental value. Moreover, for $Cu(NO_3)_2$, the computed vibrational frequencies presented in Table 3 are in excellent agreement with the experimental values reported by Rossi et al.[21]

Table 4 presents the binding energies computed with respect to the neutral fragments of the ground state structure of the complexes $Cu(NO_2)_2$, $Cu(NO_3)_2$ and $Mg(NO_2)_2$. The binding energies are computed both at the B3LYP and CCSD(T) levels. By comparing the B3LYP and CCSD(T) values obtained with the same basis set, one can observe that the computed values at the CCSD(T) level are always larger than the B3LYP ones. However, the behavior of Cu and Mg complexes is different. For $Mg(NO_2)_2$, the difference between the B3LYP and CCSD(T) values is very small while in the case of the Cu complexes, the differences are larger. As we have shown in our previous study,[20] these differences in Cu complexes are due to the different description of the first and second ionization potentials of Cu at the B3LYP and CCSD(T) levels.

Table 4 shows that the values of the metal-ligand bond dissociation energy of $CuNO_2$ and $MgNO_2$ are very similar, while the value for $CuNO_3$ is much larger. The formation of an ionic complex between two fragments, M and L, can be conceptually decomposed in two steps. The first one consists on the formation of the M^+ and L^- ions. In the second step both ions interact to yield the complex. The energy associated with the first step would be $E_i(M)$-

$E_{ea}(L)$. Table 5 shows the ionization potentials of Cu and Mg and the electron affinities of NO_2 and NO_3. It can be observed that the first ionization potentials of Mg and Cu are very similar, so that the energy necessary to ionize the fragments will be very similar in both cases. Moreover, as we have already shown,[16] the interaction energy between M^+ and L^- is also very similar in both cases. As a result, the M-NO_2 dissociation energies of $CuNO_2$ and $MgNO_2$ are quite similar. The difference between the metal-ligand bond dissociation energies of $CuNO_2$ and $CuNO_3$ can be understood from the fact that the electron affinity of NO_3 is larger than that of NO_2 (see Table 5).

For the total binding energy of the $M(NO_x)_2$ complexes, we must consider the sum of the first and second ionization potentials of the metal and twice the electron affinity of NO_x. The total M-$(NO_x)_2$ binding energies show important differences between $Cu(NO_2)_2$ and $Mg(NO_2)_2$. The reason for this difference is that the second ionization potential of Cu is much larger than the one corresponding to Mg. However, the difference between the second ionization potentials of Cu and Mg (about 100 kcal mol^{-1}) is notably larger than the difference between the total binding energy of $Cu(NO_2)_2$ and $Mg(NO_2)_2$ (less than 50 kcal mol^{-1}). This fact indicates that the M^{2+}-$2L^-$ interaction term has to be larger for $Cu(NO_2)_2$ than for $Mg(NO_2)_2$. This is mainly due to a larger ligand to metal charge transfer in the Cu complex. The Mulliken population analysis shows that the net charges on the metal in the $M(NO_2)_2$ complexes are 0.45 for Cu and 0.90 for Mg at the B3LYP level of calculation. The Cu-$(NO_3)_2$ binding energy increases with respect to the Cu-$(NO_2)_2$ value, again due to the larger electron affinity of NO_3. As a consequence of these considerations, the binding energy for the second NO_x (see Table 4) in the Cu complexes is smaller than the value for the first one, while in $Mg(NO_2)_2$ the value is much larger.

Let us now consider the basis set effect on the computed binding energies. Table 4 shows also the CCSD(T) values obtained with the larger basis set. It can be observed that the change in the metal-ligand bond dissociation energy of $M\text{-}NO_x$ is small when going from the smaller to the larger basis set. On the other hand, the values of the total binding energy of $M(NO_2)_2$ show larger differences. For $Cu(NO_2)_2$ the decrease of the energy is mainly due to the increase of the ionization potentials of Cu with the size of the basis set (see Table 5).

From this considerations, we can conclude that in Cu complexes the binding energies at B3LYP level are underestimated due to the large value of the ionization potentials of Cu. However, at CCSD(T) level the values are overestimated due to an underestimation of the ionization potential. This underestimation is partially corrected when increasing the size of the basis set, the CCSD(T) and B3LYP values approaching to each other.

Conclusions

The structure, binding energies and vibrational frequencies of the different coordination modes of $Cu(NO_2)_2$ and of the most stable structures of $Mg(NO_2)_2$ and $Cu(NO_3)_2$ have been determined. The D_{2h} structure, with the NO_2 groups showing coplanar η^2-O,O coordination, is the most stable one for $Cu(NO_2)_2$, as in the case of $Cu(NO_3)_2$ for which experimental data are available. For $Mg(NO_2)_2$ the D_{2d} structure is the most stable one. The different stability of the D_{2h} and D_{2d} structures in $Cu(NO_2)_2$ arises from the different interaction of the fragments with the d orbitals of Cu. The difference in $Mg(NO_2)_2$ is only due to steric interactions between the ligands since Mg does not have occupied d orbitals to interact with the NO_2 ligands. The computed frequencies are in good agreement with the experimental values. The binding

energies obtained at the B3LYP level with a relatively small basis set are in good agreement with the values obtained at the CCSD(T) level using a larger basis set.

Acknowledgments

This work has been financially supported by DGICYT (PB95-0640) and CIRIT (SGR95-00401). Computer time from the Centre de Supercomputació de Catalunya (CESCA) is gratefully acknowledged. L.R. gratefully acknowledges the Spanish Ministry of Education and Science for a doctoral fellowship.

References

1. See for example: (a) Veillard, A. *Chem. Rev.* **1991**, *91*, 743. (b) *Organometallic Ion Chemistry*, Ed. B. S. Freiser (Kluwer Academic Publishers, 1996).

2. Bauschlicher, C. W.; Ricca, A.; Partridge, H.; Langhoff, S. R. in *Recent Advances in Density Functional Theory*, Part II Ed. D. P. Chong, (World Scientific Publishing Company, Singapore 1997).

3. Hitchman, M. A.; Rowbottom, G. L. *Coord. Chem Rev.* **1982**, *42*, 55.

4. Herm, R: R.; Herschbach, D. R. *J. Chem. Phys.* **1970**, *52*, 5783.

5. Ham, D. O.; Kinsey, J. L. *J. Chem. Phys.* **1970**, *53*, 285.

6. Milligan, D. E.; Jacox, M. E. *J. Chem. Phys.* **1971**, *55*, 3404.

7. Goddard, J. D.; Klein, M. L. *Phys. Rev. A* **1983**, *28*, 1141.

8. Barbeschi, M.; Bencivenni, L.; Ramondo, F. *Chem. Phys.* **1987**, *112*, 387.

9. Ramondo, F. *Chem. Phys. Lett.* **1989**, *156*, 346.

10. Ramondo, F.; Bencivenni, L.; Sanna, N.; Nunziante Cesaro, S. *J. Mol. Struct. (Theochem)* **1992**, *253*, 121.

11. Lo, W.-J.; Shen, M.-y.; Yu, C.-h.; Lee, Y.-P. *J. Chem. Phys.* **1996**, *104*, 935.

12. Herm, R. R.; Lin, S. M., Mims, C. A. *J. Phys. Chem* **1973**, *77*, 2931.

13. Tevault, E.; Andrews, L. *Chem. Phys. Lett.* **1977**, *48*, 103.

14. Davis, H. F.; Suits, A. G.; Lee, Y. T. *J. Chem. Phys.* **1992**, *96*, 6710.

15. Cheong, B. S.; Parson, J. M. *J. Chem. Phys.* **1994**, *100*, 2637.

16. Rodríguez-Santiago, L.; Sodupe, M.; Branchadell, V. *J. Phys. Chem.* **1998**, *102*, 630.

17. Worden, D.; Ball, D. W. *J. Phys. Chem.* **1992**, *96*, 7167.

18. Vinckier, C.; Verhaeghe, T.; Vanhees, I. *J. Chem. Soc. Faraday Trans.* **1994**, *90*, 2003.

19. Rodríguez-Santiago, L.; Branchadell, V.; Sodupe, M. *J. Chem. Phys.* **1995**, *103*, 9738.

20. Rodríguez-Santiago, L.; Sodupe, M.; Branchadell, V. *J. Chem. Phys.* **1996**, *105*, 9966.

21. Rossi, V.; Sadun, C.; Bencivenni, L.; Caminiti, R. *J. Mol. Struct. (Theochem)* **1994**, *314*, 247.

22. La Villa, R. E.; Bauer, S. H. *J. Am. Chem. Soc.* **1963**, *85*, 3597.

23. Becke, A. D. *J. Chem. Phys.* **1993**, *98*, 5648.

24. Lee, C.; Yang, W.; Parr, R. G. *Phys. Rev. B* **1988**, *37*, 785.

25. Holthausen, M. C.; Heineman, C.; Cornehl, H. H.; Koch, W.; Schwarz, H. *J.Chem. Phys.* **1995**, *102*, 4931.

26. Raghavachari, K.; Trucks, G. W.; Pople, J. A.; Head-Gordon, M. *Chem. Phys. Lett.* **1989**, *57*, 479.

27. Dunning, T. H. *J. Chem. Phys.* **1970**. *53*, 2823.

28. Gaussian 94, Revision D.1, Frisch, M. J.; Trucks, G.W.; Schlegel, H. B.; Gill, P. M. W.; Johnson, B. G.; Robb, M. A.; Cheesman, J. R.; Keith, T. A.; Petersson, G. A.; Montgomery, J. A.; Raghavachari,K.; Al-Laham, M. A.; Zakrzewsky, V. G.; Ortiz, J. V.; Foresman, J. B.; Cioslowsky, J.; Stefanov, B.; Nanayakkara, A.; Challacombe, M.; Peng, C. Y.; Ayala, P. Y.; Chen, W.; Wong, M. W.; Andrés, J. L.; Replogle, E. S.; Gomperts, R.; Martin, R. L.; Fox, D. J.; Binkley, J. S.; Defrees, D.J.; Baker, J.; Stewart, J. J. P.; Head-Gordon, M.; Gonzalez, C.; Pople, J. A. Gaussian 94 Gaussian Inc., Pittsburgh PA, 1995.

29. A.J.H. Wachters *J. Chem. Phys.* **1970**, *52*, 1033.

30. Hay, P. J. *J. Chem. Phys.* **1977**, *66*, 4377.

31. McLean, A. D.; Chandler, G. S. *J. Chem. Phys.* **1980**, *72*, 5639.

32. Stewart, R. F. *J. Chem. Phys.* **1970**, *52*, 431.

33. MOLPRO is a package of ab initio programs written by H.-J. Werner, P. J. Knowles, with contributions from J. Almlöf, R. D. Amos, A. Berning, M. J. O. Deegan, F. Eckert, S. T. Elbert, C. Hampel, R. Lindh, W. Meyer, A. Nicklass, K. Peterson, R. Pitzer, A. J. Stone, P. R. Taylor, M. E. Mura, P. Pulay, M. Schuetz, H. Stoll, T. Thorsteinsson, and D. L. Cooper. The CCSD program is described in Hampel, C; Peterson, K.; Werner, H.-J. *Chem. Phys. Lett.*

1992, *1*, 190.

34. Kendall, R. A.; Dunning, T. H. *J. Chem. Phys.* **1992**, *96*, 6796.

35. .LaVilla, R. E.; Bauer, S. H. *J. Am. Chem. Soc.* **1963**, *85*, 3597.

36. Lafferty, W. J.; Sams, R.L.; *J. Mol. Spectry* **1977**, *66*, 478.

37. Watson, R. E.; Brodasky, T. F. *J.Chem. Phys.* **1957**, *27*, 683.

38. Moore, C. E. *Atomic Energy Levels*, Natl. Bur. Stand. Circ., U.S., No. 467 **1949**.

39. Hughes, B. M.; Lifschitz, C.; Tiernan, T. O. *J. Chem. Phys.* **1973**, *59*, 3162.

40. Bartmes, J. E. "Neutral Thermochemical Data" in *NIST Standard Reference Database Number 69*, Eds. W.G. Mallard and P.J. Linstrom, August 1997, National Institute of Standards and Technology, Gaithersburg MD, 20899 (http://webbook.nist.gov).

Table 1: Computed relative energies of the stationary points found for $Cu(NO_2)_2$.

	Symmetry	State	$[NO_2]_1$	$[NO_2]_2$	ΔE/kcalmol^{-1}
AA	D_{2h}	$^2B_{3g}$	η^2-O,O	η^2-O,O ∥	0.0
AAp	D_{2d}	$^2B_2$	η^2-O,O	η^2-O,O ⊥	23.7
AAx	D_{2h}	$^2B_{1u}$	η^2-O,O	η^2-O,O ∥	31.5
AB	C_s	$^2A'$	η^2-O,O	η^2-N,O ∥	7.5
ABp	C_s	$^2A'$	η^2-O,O	η^2-N,O ⊥	18.3[a]
AC	C_s	$^2A'$	η^2-O,O	η^1-O ∥	12.4
ACp	C_s	$^2A''$	η^2-O,O	η^1-O ⊥	17.6[a]
AD	C_{2v}	$^2A_1$	η^2-O,O	η^1-N ∥	17.9[a]
ADp	C_{2v}	$^2A_1$	η^2-O,O	η^1-N ⊥	17.4[a]
BBt	C_s	$^2A'$	η^2-N,O	η^2-N,O ∥ trans	17.1
BBi	C_{2v}	$^2B_2$	η^2-N,O	η^2-N,O ∥ cis	16.9
BC	C_s	$^2A'$	η^2-N,O	η^1-O ∥	19.4[a]
BD	C_s	$^2A'$	η^2-N,O	η^1-N ∥	20.3[a]
BDp	C_s	$^2A'$	η^2-N,O	η^1-N ⊥	20.9[a]
CCi	C_s	$^2A'$	η^1-O	η^1-O ∥ cis	19.2
CDp	C_s	$^2A'$	η^1-O	η^1-N ⊥	27.5[a]
DD	D_{2h}	^2A_g	η^1-N	η^1-N ∥	26.4[b]
DDp	D_{2d}	$^2A_1$	η^1-N	η^1-N ⊥	26.3[b]

[a]First order saddle points.

[b]Second order Saddle points

Table 2: Computed harmonic vibrational frequencies[a] for $M(NO_2)_2$, NO_2 and NO_2^- in cm^{-1}.

	NO_2 def.(B_{1u})	NO_2 def.(A_g)	NO asy. str.(B_{3g})	NO asy. str.(B_{2u})	NO sym. str.(B_{1u})	NO sym. str.(A_g)
$Cu(NO_2)_2$	882(114)	895(0)	1225(0)	1254(564)	1348(60)	1350(0)

	NO_2 def.(A_1)	NO_2 def.(B_2)	NO asy. str.(E)	NO sym. str.(B_2)	NO sym. str.(A_1)
$Mg(NO_2)_2$	882(0)	886(21)	1287(476)	1336(23)	1336(0)

	NO_2 def.(A_1)	NO sym. str.(A_1)	NO asy. str.(B_2)
NO_2	741(6)	1388(0)	1703(416)
NO_2 exp.[b]	750	1325	1634
NO_2^-	780(3)	1339(13)	1322(722)
NO_2^- exp.[c]	821	1332	1240

[a]In parenthesis, the IR intensity of each frequency in km mol^{-1}.

[b]Reference 36.

[c]Reference 37.

Table 3: Harmonic vibrational frequencies[a] for $Cu(NO_3)_2$ in cm^{-1}.

Computed[b]	exp.[c]	description
1683(0)		NO' str. ($_{Ag}$)
1668(1328)	1615	NO' str. (B_{1u})
1247(460)	1205	NO asy. str. (B_{2u})
1233(0)		NO asy. str (B_{3g})
1020(0)		NO sym. str. (A_g)
1018(65)	965	NO sym. str. (B_{1u})
778(20)		NO_3 def. (B_{3u})
777(0)		NO_3 def. (B_{2g})
774(0)		NO_2 def. (A_g)
771(111)		NO_2 def. (B_{1u})

[a]In parenthesis, the IR intensity of each frequency in km mol^{-1}.

[b]O' indicates the terminal oxygen of the NO_3 fragments.

[c]Reference 21.

Table 4: Metal-ligand binding energies of $M(NO_x)_n$ complexes (in kcal mol^{-1}) computed at different levels of calculation.

	successive				total	
	$M\text{-}NO_x$		$MNO_x\text{-}NO_x$		$M\text{-}(NO_x)_2$	
	B3LYP	CCSD(T)[a]	B3LYP	CCSD(T)[a]	B3LYP	CCSD(T)[a]
$Cu(NO_2)_2$	49.2	57.2(56.1)	37.4	43.8(36.9)	86.6	101.0(93.9)
$Cu(NO_3)_2$	72.3	83.9(85.2)	71.6	75.9	143.9	159.8
$Mg(NO_2)_2$	47.2	49.2(51.5)	88.5	93.5(96.1)	135.7	142.7(147.6)

[a]In parentheses are shown the CCSD(T) values with the larger basis set.

Table 5: Computed ionization potential for the metals and adiabatic electron affinities of NO_x.

	metal E_I/eV		
	B3LYP	CCSD(T)[a]	exp.
Cu	8.03	7.06(7.15)	7.73[b]
Cu^+	20.80	19.62(20.00)	20.29[b]
Mg	7.73	7.54(7.58)	7.65[b]
Mg^+	15.46	14.80(14.87)	15.03[b]
	NO_x E_{ea}/eV		
NO_2	2.36	2.12(2.13)	2.28[c]
NO_3	4.04	3.82(3.92)	3.92±0.2[d]

[a]In parentheses are shown the CCSD(T) values with the larger basis set.

[b]Reference 38.

[c]Reference 39.

[d]Reference 40.

Figure captions

Figure 1: Coordination modes of one NO_2 to the metal atom.

Figure 2: Computed structures of the different energy minima determined for the $Cu(NO_2)_2$ complex. Distances are in Angstroms and angles in degrees.

Figure 3: Diagram of the most important orbitals involved in the formation of the D_{2h} and D_{2d} structures of $Cu(NO_2)_2$.

Figure 4: Computed D_{2d} and D_{2h} structures $Mg(NO_2)_2$. Distances are in Angstroms and angles in degrees.

Figure 5: Computed D_{2h} structure of $Cu(NO_3)_2$. In parentheses are shown the experimental values[35]. Distances are in Angstroms and angles in degrees.

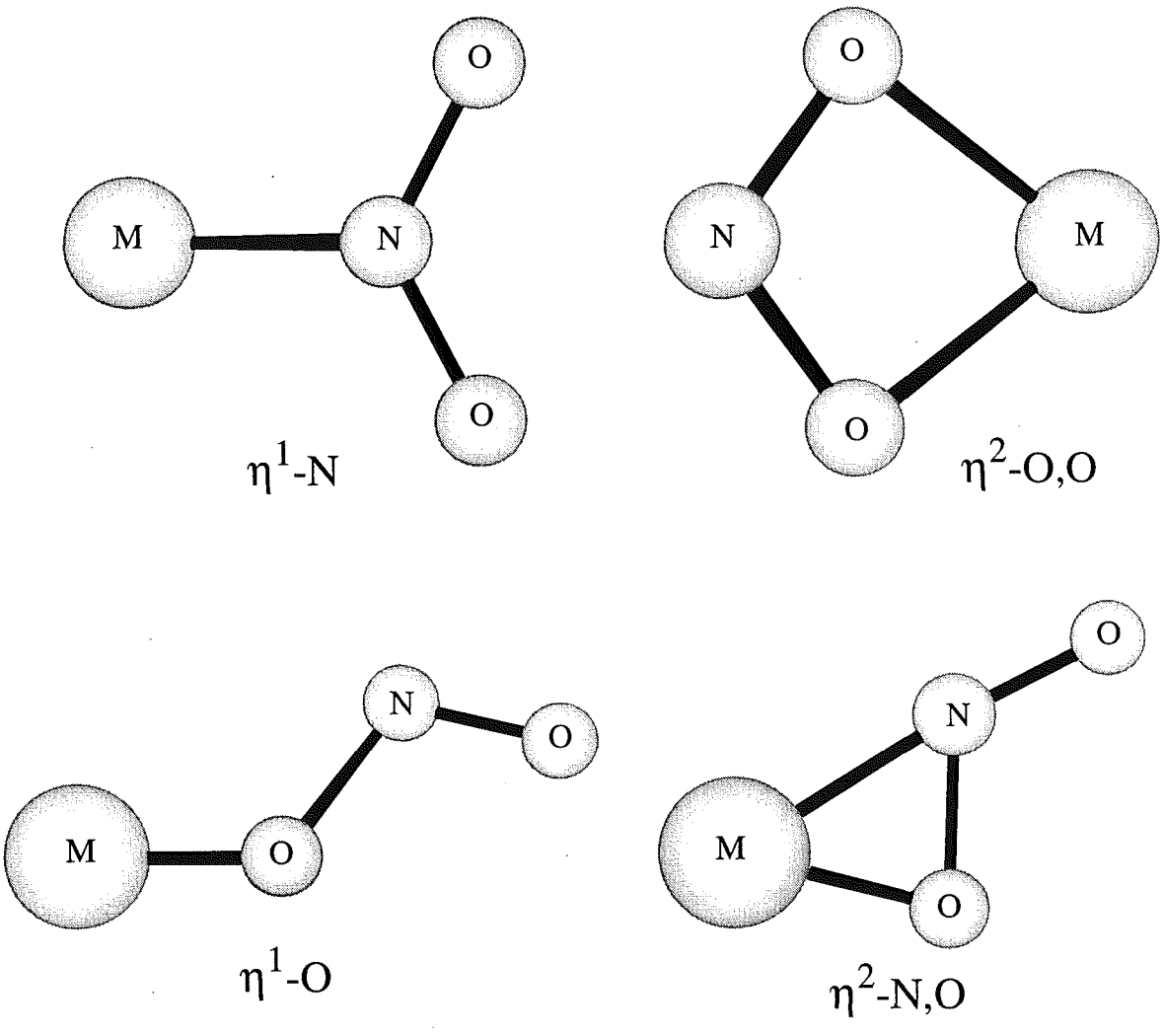

Figure 1

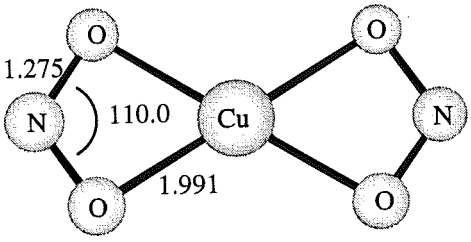

AA

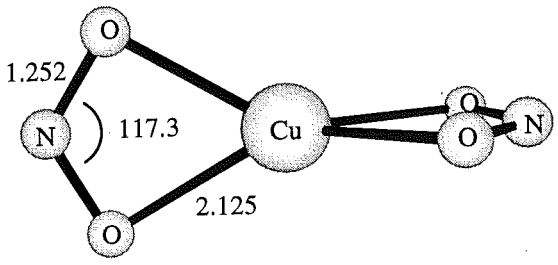

AAp

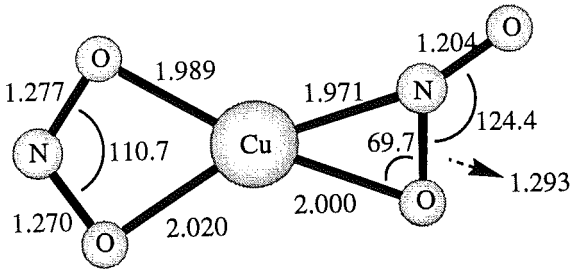

AB

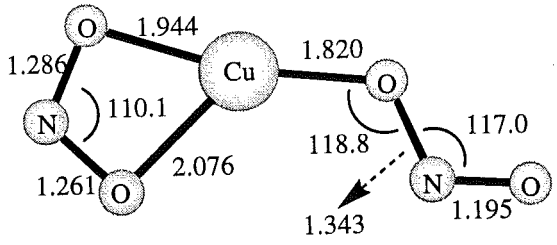

AC

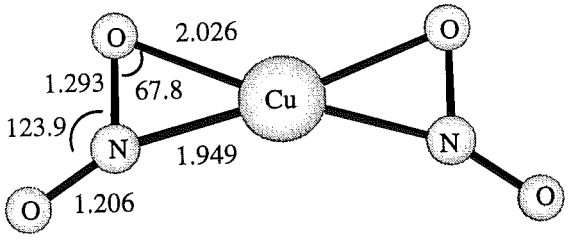

BBi

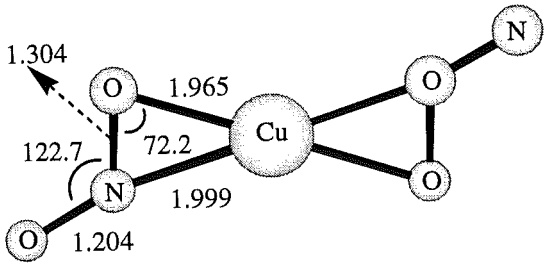

BBt

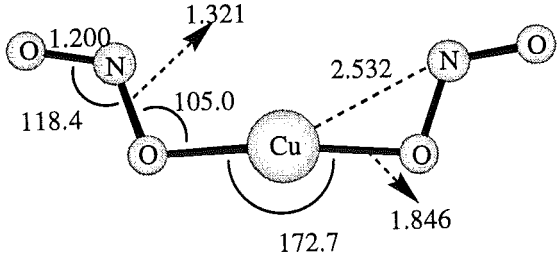

CCi

Figure 2

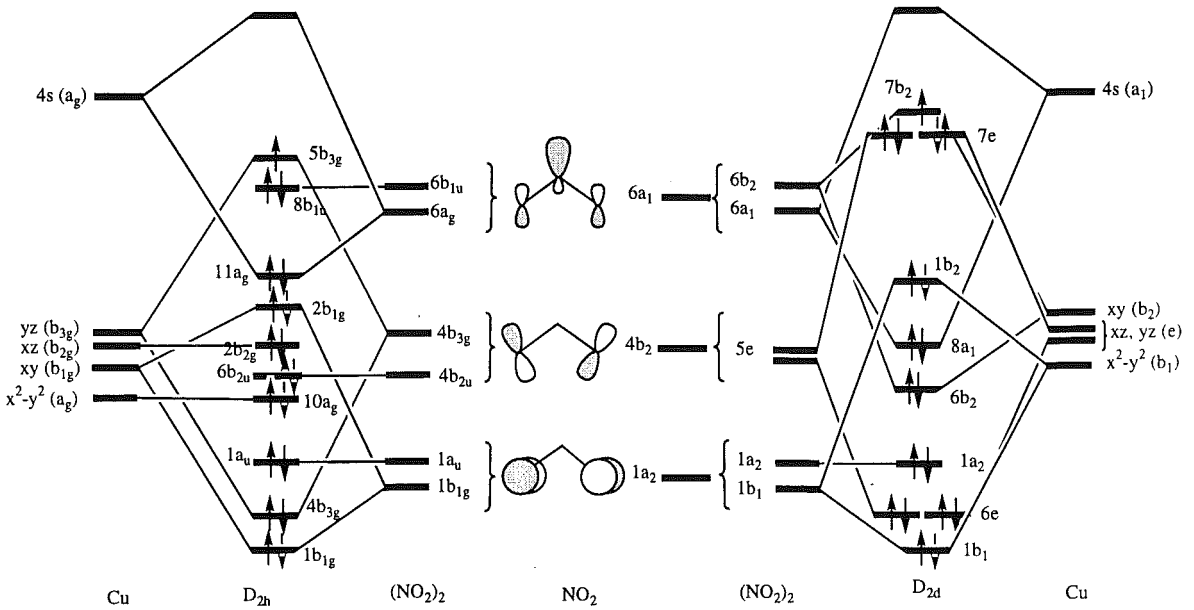
4s (a_g)
5b_{3g}
8b_{1u}
6b_{1u}
6a_g
11a_g
2b_{1g}
4b_{3g}
yz (b_{3g})
xz (b_{2g})
xy (b_{1g})
x^2-y^2 (a_g)
2b_{2g}
6b_{2u}
4b_{2u}
10a_g
1a_u
1b_{1g}
4b_{3g}
1b_{1g}
6a_1
4b_2
1a_2
6b_2
6a_1
5e
1a_2
1b_1
7b_2
7e
1b_2
8a_1
6b_2
1a_2
6e
1b_1
4s (a_1)
xy (b_2)
xz, yz (e)
x^2-y^2 (b_1)
Cu
D_{2h}
$(NO_2)_2$
NO_2
$(NO_2)_2$
D_{2d}
Cu

Figure 3

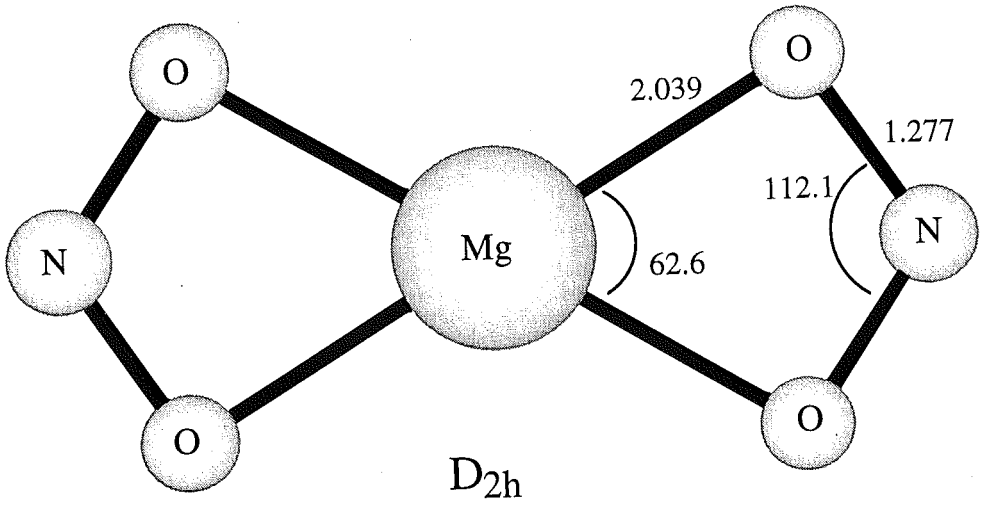

D_{2h}

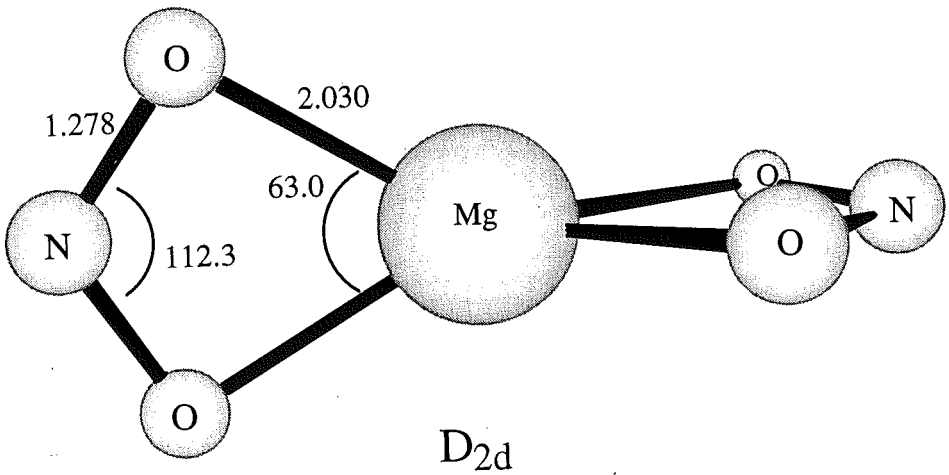

D_{2d}

Figure 4

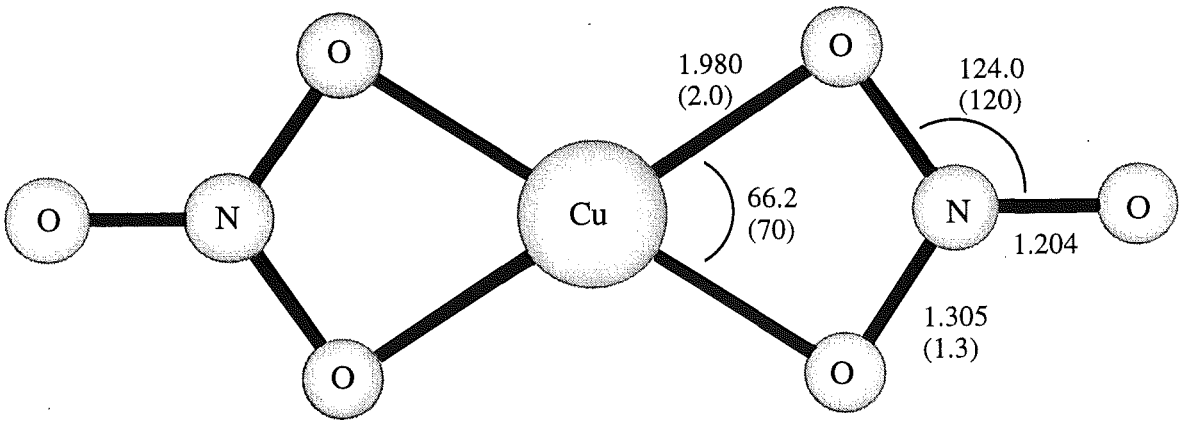

Figure 5

7. "Coordination of Cu^+ Ions to Zeolite Frameworks Strongly Enhances their Ability to Bind NO_2. An ab initio Density Functional Study"

J. Am. Chem. Soc. 1998, 120, 1545−1551 1545

Coordination of Cu^+ Ions to Zeolite Frameworks Strongly Enhances Their Ability To Bind NO_2. An ab Initio Density Functional Study

Luis Rodriguez-Santiago,[†] Marek Sierka,[‡] Vicenç Branchadell,[†] Mariona Sodupe,[†] and Joachim Sauer*,[‡]

Contribution from the Departament de Química, Universitat Autònoma de Barcelona, Edifici Cn, 08193 Bellaterra, Spain, and Max-Planck-Gesellschaft, Arbeitsgruppe Quantenchemie an der Humboldt-Universität, D-10117 Berlin, Germany

Received September 11, 1997. Revised Manuscript Received December 5, 1997

Abstract: Comparison is made of the interaction of NO_2 with Cu^+ ions in the gas phase and inside zeolites using density functional theory (B3LYP functional). The zeolite is represented by a tritetrahedra model embedded in the periodic structure of zeolite ZSM-5 and by a free space cluster model. Both models yield virtually the same results. Cu^+ is coordinated to two oxygen atoms of the zeolite framework only. For the complexes with NO_2, several minima and transition structures on the potential energy surfaces are localized. The naked Cu^+ ion preferentially binds NO_2 in the η^1-O trans mode, while in zeolites the Cu^+ site binds NO_2 in a $^2\eta$-O,O coordination. For the $^2\eta$-O,O structure the binding is three to four times stronger in the zeolite (43 kcal/mol) than in the gas phase which is due to a three-body zeolite framework−Cu^+ ion−NO_2 interaction. d^{10}−s^1d^9 promotion leads to a more favorable orbital interaction between Cu^+ and NO_2 in the $^2A''$ state and, due to reduced repulsion, to a stronger electrostatic interaction between Cu^+ and the zeolite framework.

1. Introduction

Transition metal cations show catalytic activity in different systems ranging from heterogeneous over homogeneous to biological. In recent years, it became possible to study the reactivity of naked (noncoordinated) transition metal cations.[1] Despite a fascinating chemistry revealed by these studies, catalytic activity could be observed in exceptional cases only, see, e.g., refs 2 and 3 An example is the role that Cu^+ ions play in the catalytic decomposition of NO_x—a mixture of NO and NO_2 of obvious environmental significance. Cu-exchanged zeolites, in particular Cu−ZSM-5, show a high and sustained activity.[4] Many studies reached the conclusion that the Cu^+ ion is in the core of the active sites of these catalysts.[5−8] In contrast, Schwarz and co-workers did not find any catalytic activity when investigating the [Cu^+, N, O] system in the gas phase.[9] This highlights the important role that ligands play in activating transition metal cations.

Some activation of Cu^+ and other transition metal ions by ligands has been observed before. The second water ligand was found to bind more strongly than the first one,[10] in contrast to alkaline metal ions, for which the energies for adding the next ligand are steadily decreasing when adding an increasing number of ligands. Confirmation came from ab initio calculations[11−13] which also provided the explanation:[12] "The unique feature of transition metal ions is their ability to reduce metal−ligand repulsion by sdσ hybridization. Since sdσ hybridization reduces the charge density along the σ axis, the second ligand binding energy can be larger than the first, because both ligands benefit from reduced repulsion while sharing the energetic cost of hybridization." We will show below that the much stronger activation of Cu^+ ions by zeolite frameworks has a similar origin.

We study the interaction of NO_2 with Cu^+ ions in the gas phase and in zeolites. We localize several stationary points on the potential energy surfaces by ab initio methods employing density functional theory (DFT). We find a dramatic increase of the binding energy of NO_2 on the Cu^+ ion inside the zeolite compared with the naked Cu^+ ion. For a realistic description of this effect it is vital to have a valid model of the active site. In agreement with previous theoretical studies[14,15] we find that the Cu^+ ion is coordinated to two lattice oxygen atoms of the zeolite framework only, in contrast to the Cu^{2+} ion which prefers a higher coordination. Two is an unusually low coordination number for Cu^+, but it is confirmed by EXAFS studies on activated Cu-exchanged zeolites.[16,17] Our description includes

* Corresponding author: Humboldt Universität, Arbeitsgruppe Quantenchemie, Sitz: Jägerstrasse 10-11, D-10117 Berlin. E-mail: js@qc.ag-berlin.mpg.de.

[†] Universitat Autònoma de Barcelona.

[‡] Humboldt-Universität.

(1) Eller, K.; Schwarz, H. *Chem. Rev. (Washington, D.C.)* **1991**, *91*, 1121.

(2) Wesendrup, R.; Schröder, D.; Schwarz, H. *Angew. Chem., Int. Ed. Engl.* **1994**, *33*, 1174.

(3) Pavlov, M.; Blomberg, M. R. A.; Siegbahn, P. E. M.; Wesendrup, R.; Heinemann, C.; Schwarz, H. *J. Phys. Chem. A* **1997**, *101*, 1567.

(4) Shelef, M. *Chem. Rev. (Washington, D.C.)* **1995**, *95*, 209.

(5) Iwamoto, M.; Yahiro, H.; Tanda, K.; Mizuno, N.; Mine, Y.; Kagawa, S. *J. Phys. Chem.* **1991**, *95*, 3727.

(6) Li, Y.; Hall, W. K. *J. Catal.* **1991**, *129*, 202.

(7) Spoto, G.; Zecchina, A.; Bordiga, S.; Ricchiardi, G.; Martra, G.; Leofanti, G.; Petrini, G. *Appl. Catal. B: Environmental* **1994**, *3*, 151.

(8) Wichterlová, B.; Dědeček, J.; Sobalík, Z.; Vondrová, A.; Klier, K. *J. Catal.* **1997**, *169*, 194.

(9) Sülzle, D.; Schwarz, H.; Moock, K. H.; Terlouw, J. K. *Int. J. Mass Spectrom. Ion Proc.* **1991**, *108*, 269.

(10) Magnera, T. F.; David, D. E.; Stuhlik, D.; Orth, R. G.; Jonkman, H. T.; J. Michl *J. Am. Chem. Soc.* **1989**, *111*, 5036.

(11) Bauschlicher, C. W. J.; Langhoff, S. R.; Partridge, H. In *Organometallic Ion Chemistry*; Freiser, B. S., Ed.; Kluwer Academic Press: 1996; p 47.

(12) Bauschlicher, C. W. J.; Langhoff, S. R.; Partridge, H. *J. Chem. Phys.* **1991**, *94*, 2068.

(13) Rosi, M.; Bauschlicher, C. W. *J. Chem. Phys.* **1989**, *90*, 7264.

(14) Trout, B. L.; Chakraborty, A. K.; Bell, A. T. *J. Phys. Chem.* **1996**, *100*, 17582.

(15) Blint, R. J. *J. Phys. Chem.* **1996**, *100*, 19518.

S0002-7863(97)03196-X CCC: $15.00
Published on Web 02/06/1998

1546 J. Am. Chem. Soc., Vol. 120, No. 7, 1998 Rodriguez-Santiago et al.

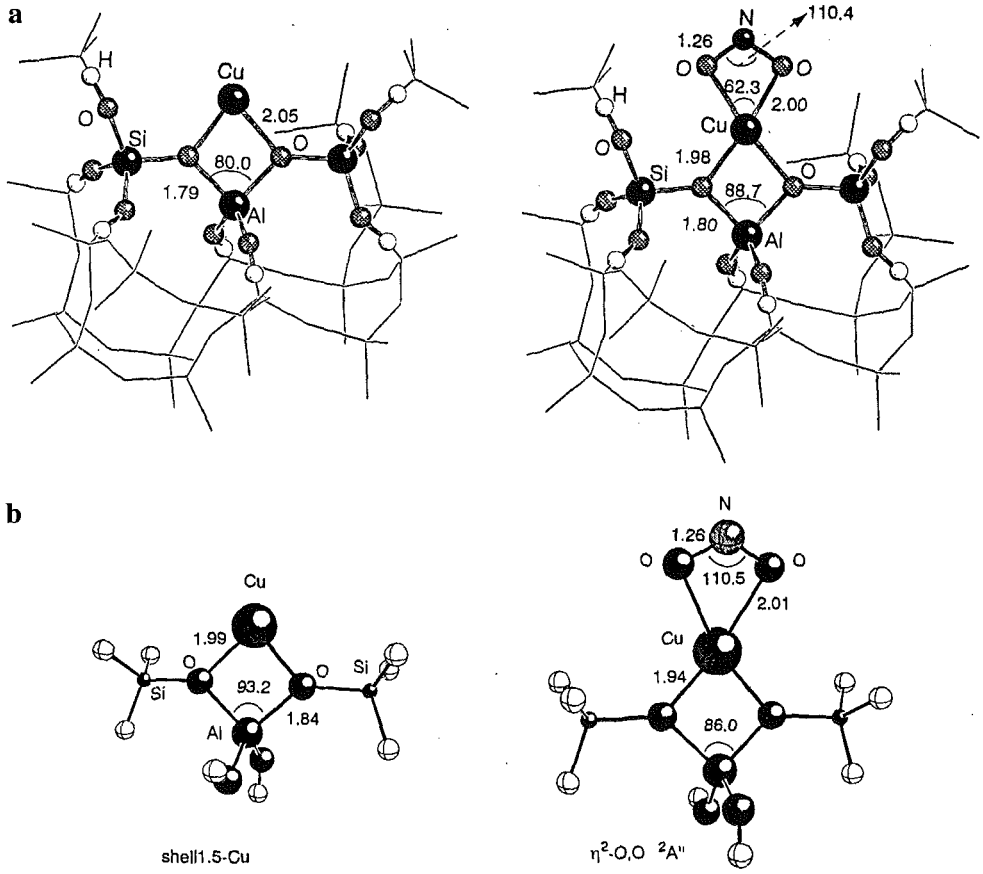

Figure 1. Predicted structures for the Cu^+ site in zeolites (left) and for its complex with NO_2 (right): (a) tritetrahedra model embedded into the periodic ZSM-5 structure and (b) zeolite framework represented by the shell-1.5 model.

the full periodic structure of the MFI framework (MFI is the common code for the framework type of ZSM-5 catalysts) for which we adopt the shell-model ion pair potential. We then determine the local structure of the Cu^+ site by embedding a model consisting of three tetrahedra (Figure 1a) into the periodic MFI structure and treat it quantum mechanically. We use for this purpose a recently developed combined quantum mechanics/interatomic potential approach (QM-pot).[18,19] We finally show that a virtually identical structure of the active site is obtained when using a nonembedded cluster model consisting of a central AlO_4^- tetrahedron and two neighbored SiO_4 tetrahedra (Figure 1b). This model, shell-1.5, proved successful in previous studies[20,21] and is used for the majority of structure predictions of the complexes of NO_2 with Cu^+ in zeolites. We finally show that the effect of the zeolite framework as ligand is special. The increase of the binding energy predicted for the zeolite is by far larger than that predicted for Cu^+ with two water molecules as ligands, even if we simulate the spatial arrangement of the two oxygen binding sites of zeolite frameworks by constraining the two water ligands to a bent configuration.

There is an increasing number of experimental and theoretical studies of the direct catalytic decomposition and the selective catalytic reduction of NO_x. This is not the place to give a complete account, nor it is our aim to study the whole mechanism. We focus here on NO_2, which is of interest not only as a pollutant itself but also as the product of the catalytic oxidation of NO.[22] Moreover, among several proposed mechanisms for the NO direct decomposition, the formation of the $ZCu{\cdot}NO_2$ complex has been suggested by several authors.[7,23,24] It can react with NO to form the $ZCu(NO_2)NO$ intermediate which decomposes into molecular nitrogen and oxygen.

Among the computational studies devoted to the problem[14,15,25–32] two are of particular relevance to our study. The DFT study of Yokomichi et al. compares the binding of NO to the naked Cu^+ ion and to the $[(HO)_2Al(OH)_2]^-Cu^+$ model for the Cu^+ site in zeolites.[30] They find enhanced binding although by far not as dramatic as found for NO_2 in the present study. They explain the effect by destabilization of d-orbitals due to interactions with the oxygen atoms of the zeolite skeleton. As

(16) Lamberti, C.; Bordiga, S.; Salvalaggio, M.; Spoto, G.; Zecchina, A.; Geobaldo, F.; Vlaic, G.; Bellatreccia, M. *J. Phys. Chem. B* **1997**, *101*, 344.
(17) Yamashita, H.; Matsuoka, M.; Tsuji, K.; Shioya, Y.; Anpo, M.; Che, M. *J. Phys. Chem.* **1996**, *100*, 397.
(18) Eichler, U.; Kölmel, C.; Sauer, J. *J. Comput. Chem.* **1996**, *18*, 463.
(19) Brändle, M.; Sauer, J. *J. Mol. Catal. A: Chem.* **1997**, *119*, 19.
(20) Haase, F.; Sauer, J. *J. Am. Chem. Soc.* **1995**, *117*, 3780.
(21) Krossner, M.; Sauer, J. *J. Phys. Chem.* **1996**, *100*, 6199.
(22) Shelef, M.; Montreuil, C. N.; Jen, H. W. *Catal. Lett.* **1994**, *26*, 277.
(23) Valyon, J.; Hall, W. K. *J. Catal.* **1993**, *143*, 520.
(24) Giamello, E.; Murphy, D.; Magnacca, G.; Morterra, C.; Shioya, Y.; Nomura, T.; Anpo, M. *J. Catal.* **1992**, *136*, 510.
(25) Hass, C.; Schneider, W. F. *J. Phys. Chem.* **1996**, *100*, 9292.
(26) Schneider, W. F.; Hass, K. C.; Ramprasad, R.; Adams, J. B. *J. Phys. Chem.* **1996**, *100*, 6032.
(27) Schneider, W. F.; Hass, K. C.; Ramprasad, R.; Adams, J. B. *J. Phys. Chem.* **1997**, *101*, 4353.
(28) Trout, B. L.; Chakraborty, A. K.; Bell, A. T. *J. Phys. Chem.* **1996**, *100*, 4173.
(29) Yokomichi, Y.; Ohtsuka, H.; Tabata, T.; Okada, O.; Yokoi, Y.; Ishikawa, H.; Yamaguchi, R.; Matsui, H.; Tachibana, A.; Yamabe, T. *Catal. Today* **1995**, *23*, 431.
(30) Yokomichi, Y.; Yamabe, T.; Ohtsuka, H.; Kakumoto, T. *J. Phys. Chem.* **1996**, *100*, 14424.
(31) Ramprasad, R.; Schneider, W. F.; Hass, K. C.; Adams, J. B. *J. Phys. Chem.* **1997**, *101*, 1940.
(32) Brand, H. V.; Redondo, A.; Hay, P. J. *J. Phys. Chem. B* **1997**, *101*, 7691.

part of their comprehensive analysis of possible intermediates in the NO_x decomposition process, Trout et al. study several isomers of the complex of NO_2 with a model of the Cu^+ ion in ZSM-5.[14] Their and our results for the structures and binding energies are remarkably similar, although there are some differences in the method used and the model adopted. Trout et al. use the local density approximation (LDA) and a different basis set. Their cluster model has the central AlO_4 tetrahedron surrounded by four SiO_4 tetrahedra, and the terminating OH groups are fixed at observed atomic positions.

2. Details of Calculations

DFT (density functional theory) calculations have been performed using the B3LYP functional which proved successful for a broad class of problems including transition metals[3,33-35] and which is a major improvement compared to LDA. The following basis sets optimized by Ahlrichs and co-workers have been adopted:[36] Cu – double-ζ augmented with a p function (exponent 0.155 065), i.e., [8s,6p,3d]; NO_2 – triple-ζ; zeolite models – triple-ζ on oxygen and double-ζ on all other atoms. Polarization functions with exponents 0.35, 0.30, 1.2, 1.0, and 0.8 are added to all Si, Al, O, N, and H atoms, respectively. DFT calculations are made using the TURBODFT code.[37] The coupled cluster CCSD(T) calculations follow in all details the description in ref 35 and use the GAUSSIAN code.[38]

Our calculations on the $Cu^+(H_2O)$ and $Cu^+(H_2O)_2$ complexes yield 43.8 and 44.6 kcal/mol for the binding of the first and second water ligand, respectively—slightly larger values than computed with the MCPF method by Bauschlicher et al. (40.5 and 41.3 kcal/mol)[12] or than inferred from experiments by Mangera et al. (35 ± 3 and 39 ± 3 kcal/mol).[10] We correctly reproduce the increased binding energy for the second ligand.

For describing the periodic zeolite structure both in the combined QM-pot approach and in the pure potential function energy minimizations the shell-model ion pair potential[39] is used. The combined QM-pot calculations make use of the TURBODFT[37] and the GULP[40] codes in the quantum and the shell-model ion pair potential part, respectively. The parameters for the ions of the anionic zeolite framework have been found by a fit to DFT data obtained with the same basis set as used here.[41] The parameters for Cu^+ are taken from ref 42. The parameters used are summarized in the Supporting Information.

3. Results and Discussion

3.1. Structure of the Cu^+ Site. First we performed a lattice energy minimization using the shell-model ion pair potential alone to determine the structure of the Cu^+ site in a periodic ZSM-5 environment. One Al atom per unit cell was substituted into the T12 position of the orthorhombic structure of MFI (96 TO_2 formula units, hence the Si/Al ratio is 95).[43] This position was also considered before,[14] and there is no reason to believe that the results will critically depend on the substitution site. It was found that the relative energies differ by no more than 5 kcal/mol when substituting Al in any of the 24 different sites. The T12 site was found only about 2.5 kcal/mol above the minimum energy substitution site. The lattice energy minimization was made in P1 symmetry and resulted in a monoclinic structure. The Cu^+ ion is found coordinated to two lattice oxygen atoms only. Even if the optimization was started with structures in which the Cu^+ ion was inside a five-membered ring the same 2-fold coordinated structure was found. Our observations are slightly at variance with the report of Sayle et al.[44] A more comprehensive simulation of a large variety of different Cu sites in ZSM-5 by a shell-model potential with parameters slightly different from ours also yielded dicoordinated Cu^+ sites, but the majority of Cu^+ sites had a larger coordination number. Note that the simulations of Sayle et al. also allowed OH^- species to coordinate to the Cu^+ ion.

Next we defined a tritetrahedra cluster (T3), $[(HO)_3SiO\text{-}Al(OH)_2OSi(OH)_3]^-$, around the Cu^+ site (Figure 1a), and a structure refinement was made using the combined QM-pot approach. The 2-fold coordination remained unchanged, and the $Cu^+\cdots Al$ and $Cu^+\cdots O$ distances changed to 2.8 and 2.05 Å, respectively. Trout et al. also found a 2-fold coordinated structure with slightly shorter bond distances. The $Al\cdots O$ distance was 2.4 Å, and two slightly different $Cu^+\cdots O$ bond distances of 1.95 and 1.86 Å were obtained. Hartree–Fock calculations on cluster models[15] also yield a 2-fold coordination of Cu^+ with $Cu^+\cdots O$ distances of 2.10 and 2.16 Å. These results are in agreement with the experimental structure information available. From $^{27}Al-^{65}Cu$ SEDOR NMR experiments on Cu–ZSM5 a Cu–Al distance of 2.3 ± 0.2 Å has been inferred.[45] The EXAFS experiments of Yamashita et al.[17] and Lamberti et al.[16] yield Cu–O distances of 1.94 and 2.00 Å, respectively. Other EXAFS and XANES data imply a coordination number of 2.1 and a mean Cu–O distance of 1.94 Å.[46,47]

Figure 1b shows the structure of the CuZ site obtained by DFT calculations when the zeolite is represented by the shell-1.5 model. The binding energy of Cu^+ to the shell-1.5 model is 160 kcal/mol. This model is OH terminated at the central Al atom, but H-terminated at the Si atoms. The tri-tetrahedra model adopted in the embedded cluster calculation is OH terminated on both the Al and the Si atoms. There is good agreement between this free cluster optimization and the embedded cluster calculations. Embedding has two effects. It constraints the relaxation of the cluster atoms (since they "feel" that they are part of the zeolite framework) and it adds long-range interactions. Comparison of parts a and b of Figure 1 shows that this has little effect on the coordination type and on the strength of the interaction. The $Cu^+\cdots O$ distances shrink by 2–3% only. We conclude that the shell-1.5 model without embedding provides a reasonable first information on the effect of coordinating the Cu^+ ion to the MFI framework.

(33) Bauschlicher, C. W.; Ricca, A.; Partridge, H.; Langhoff, S. R. In *Recent Advances in Density Functional Theory, Part II*; Chong, D. P., Ed.; World Scientific Publishing Company: Singapore, 1997.
(34) Holthausen, M. C.; Heineman, C.; Cornehl, H. H.; Koch, W.; Schwarz, H. *J. Chem. Phys.* **1995**, *102*, 4931.
(35) Rodriguez-Santiago, L.; Sodupe, M.; Branchadell, V. *J. Chem. Phys.* **1996**, *105*, 9966.
(36) Schäfer, A.; Horn, H.; Ahlrichs, R. *J. Chem. Phys.* **1992**, *97*, 2571.
(37) Treutler, O.; Ahlrichs, R. *J. Chem. Phys.* **1995**, *102*, 346.
(38) Head-Gordon, M.; Gill, P. M. W.; Wong, M. W.; Foresman, J. B.; Johnson, B. G.; Schlegel, H. B.; Robb, M. A.; Replogle, E. S.; Gomperts, R.; Andres, J. L.; Raghavachari, K.; Binkley, J. S.; Gonzalez, C.; Martin, R. L.; Fox, D. J.; Defrees, D. J.; Baker, J.; Stewart, J. J. P.; Pople, J. A. *GAUSSIAN 92*; Gaussian, Inc.: Pittsburgh, PA, 1992.
(39) Dick, B. G. J.; Overhauser, A. W. *Phys. Rev.* **1958**, *112*, 90.
(40) Gale, J. D. *J. Chem. Soc., Faraday Trans.* **1997**, *93*, 629.
(41) Sierka, M.; Sauer, J. *Faraday Discuss.* **1997**, *106*, 41.
(42) Sayle, D. C.; Perrin, M. A.; Nortier, P.; Catlow, C. R. A. *J. Chem. Soc., Chem. Commun.* **1995**, 945.
(43) van Koningsveld, H.; Jansen, J. C.; Bekkum, H. v. *Zeolites* **1990**, *10*, 235.
(44) Sayle, D. C.; Catlow, C. R. A.; Gale, J. D.; Perrin, M. A.; Nortier, P. *J. Phys. Chem.* **1997**, *101*, 3331.
(45) Hu, S.; Reimer, J. A.; Bell, A. T. *J. Phys. Chem.* **1997**, *101*, 1869.
(46) Liu, D. J.; Robota, H. J. *Appl. Catal. B* **1994**, *4*, 155.
(47) Liu, D.-J.; Robota, H. J. In *Reduction of Nitrogen Oxide Emissions*; ACS Symposium Series, Vol. 587 Ozkan, U.S., Agarwal, S. K., Marcelin, G., Eds.; American Chemical Society: Washington, DC, 1995; p 147.
(48) Ehrhardt, C.; Ahlrichs, R. *Theor. Chim. Acta* **1985**, *68*, 231.

Table 1. Binding Energies of NO_2 (kcal/mol), Relative Energies w.r.t. the Most Stable Structure Are Given in Parentheses

		$[Cu{\cdot}NO_2]^+$ this work			$ZCu{\cdot}NO_2$ this work	$ZCu{\cdot}NO_2$ ref 14
structure		CCSD(T)//B3LYP	B3LYP		B3LYP	LSD
η^1—O trans		19.6 (0.0)	26.4 (0.0)		30.3 (12.4)	
η^1—O cis		17.1 (2.4)	24.3 (2.1)		30.0 (12.7)	12.2 (30.4)
η^1—N		7.7 (11.9)	16.4 (10.0)		25.1 (17.6)	26.8 (15.8)
η^2—N,O		7.1 (12.5)	16.4 (10.0)		35.8 (6.9)	
η^2—O,O	$^2A_1$	10.4 (9.1)	14.0 (12.4)	$^2A'$	10.7(32.0)	
	$^2B_2$		10.5 (15.9)	$^2A''$	42.7 (0.0)	42.6 (0.0)

Table 2. Results of Mulliken Population Analysis and, in Parentheses, a Population Analysis Based on Occupation Numbers (Ref 48)

			charge		spin density		metal orbital population		
			Cu	NO_2	Cu	NO_2	s	p	d
	ZCu		0.57 (1.02)				6.34	12.24	9.85
η^2—O,O	Cu^+NO_2	$^2A_1$	0.83 (0.99)	0.18 (0.01)	0.13 (0.05)	0.87 (0.93)	6.14	12.07	9.96
	$ZCuNO_2$	$^2A'$	0.72 (1.13)	−0.25 (−0.30)	0.53 (0.75)	0.38 (0.34)	6.47	12.33	9.47
	Cu^+NO_2	$^2B_2$	0.87 (0.82)	0.13 (0.18)	0.40 (0.40)	0.60 (0.60)	6.42	12.16	9.55
	$(H_2O)_2Cu^+NO_2$	$^2A''$	0.70	−0.13	0.58	0.35	6.54	12.37	9.37
	$ZCuNO_2$	$^2A''$	0.68 (0.91)	−0.32 (−0.35)	0.63 (0.62)	0.20 (0.20)	6.57	12.42	9.33
η^2—N,O	Cu^+NO_2	$^2A'$	0.85 (0.87)	0.15 (0.13)	0.23 (0.35)	0.77 (0.65)	6.23	12.08	9.83
	$ZCuNO_2$		0.67 (0.83)	−0.26 (−0.27)	0.50 (0.49)	0.36 (0.37)	6.50	12.41	9.43

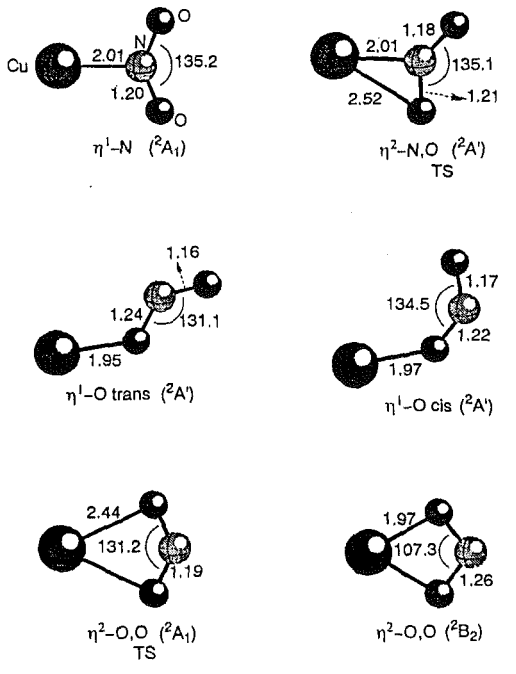

Figure 2. Predicted structures of different isomers and electronic states of the Cu^+-NO_2 gas-phase complex.

3.2. Structure and Stability of Cu^+NO_2 Gas-Phase Complexes. Figure 2 and Table 1 show the DFT(B3LYP) results for the different structure isomers of NO_2 interacting with Cu^+ in the gas phase and for the stabilization energies. Different coordination modes have been found: the bidentate η^2-O,O and η^2-N,O coordinations and the monodentate η^1-O (cis and trans) and η^1-N coordinations. Only the η^1-O and η^1-N modes are minima on the ground-state potential energy surface. The most stable isomer is η^1-O (trans), with η^1-O (cis) being only 2.1 kcal/mol higher in energy. The η^2-O,O structure ($^2A_1$ state) is the transition state connecting the two equivalent η^1-O cis isomers, while the η^2-N,O one corresponds to the η^1—O (trans) → η^1—N isomerization. The η^1-N structure is a very shallow minimum with almost the same energy as the η^2-N,O transition structure. Comparison is made with CCSD(T) single point results. The binding energies are reduced in all cases, but the relative stability of the local minima is maintained and the transition structures remain above the minima they connect.

The bonding in the ground state ($^2A'$ and $^2A_1$) is mainly noncovalent and arises from the interaction of the $^1S(d^{10})$ state of Cu^+ and the $^2A_1$ ground state of NO_2. The relative stability of the different isomers can be understood in terms of metal—ligand repulsion and electrostatic attraction. Table 2 shows for the η^2-O,O and η^2-N,O transition structures that—in agreement with this view—the metal orbital population stays close to $d^{10}s^0$, the unpaired electron remains localized on NO_2, and the positive excess charge remains on Cu. Consistently, the structure of the NO_2 fragment in the complex is very similar to that of the $^2A_1$ state of free NO_2 at the same level of calculation (Table 3).

The $^2B_2$ state of the η^2-O,O coordination is a minimum on an excited potential energy surface. It can be viewed as the interaction of the $^1S(d^{10})$ state of Cu^+ with the $^2B_2$ state of NO_2. The geometric structure of the NO_2 fragment in this state is very similar to that of the $^2B_2$ state of free NO_2 (Table 3). The left-hand side of Figure 3 shows the most relevant orbitals involved in the bond between Cu^+ and NO_2. The orbital occupation is given for the $^2A_1$ ground state of NO_2. In the $^2B_2$ excited state the $4b_2$ orbital is singly occupied, while the $6a_1$ orbital is doubly occupied. This opens the possibility for an electron donation from the doubly occupied $6a_1$ orbital of

(49) Morino, Y.; Tanimoto, M.; Saito, S.; Hirota, E.; Awata, R.; Tanaka, T. *J. Mol. Spectrosc.* **1983**, *98*, 331.
(50) Kaldor, U. *Chem. Phys. Lett.* **1991**, *185*, 131.
(51) Ervin, K. M.; Ho, J.; Lineberger, W. C. *J. Phys. Chem.* **1988**, *92*, 5405.
(52) Hughes, B. M.; Lifschitz, C.; Tiernan, T. O. *J. Chem. Phys.* **1973**, *59*, 3162.

Table 3. Bond Distance (Å) Bond Angle (deg), and Electron Affinity (EA, eV) for NO_2[e]

		r(NO)	∠ONO	EA
NO_2	$^2A_1$	1.194	134.2	
	obsd	(1.194)[a]	(133.9)[a]	
	$^2B_2$	1.254	101.7	
	calcd	(1.270)[b]	(100.6)[b]	
NO_2^-	$^1A_1$	1.264	116.0	1.85
	obsd	(1.25 ± 0.02)[c]	(117.5 ± 2.0)[c]	(2.28)[d]

[a] Reference 49. [b] CCSD method, ref 50. [c] Reference 51. [d] Reference 52. [e] Observed results or other computed results in parentheses.

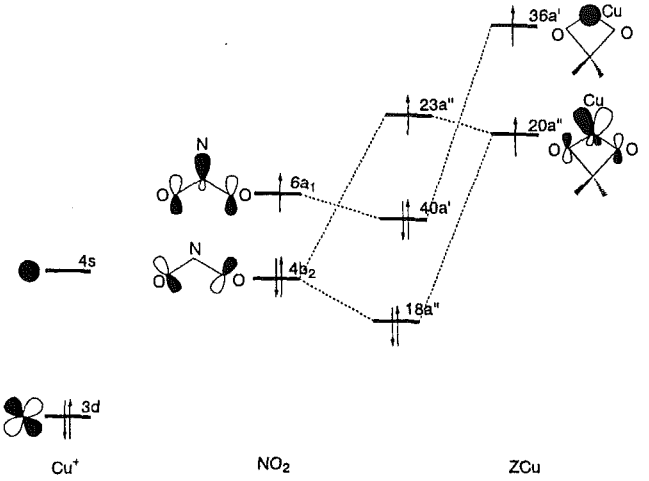

Figure 3. Diagram of the most important orbitals involved in the formation of the bond between the Cu^+ site and NO_2.

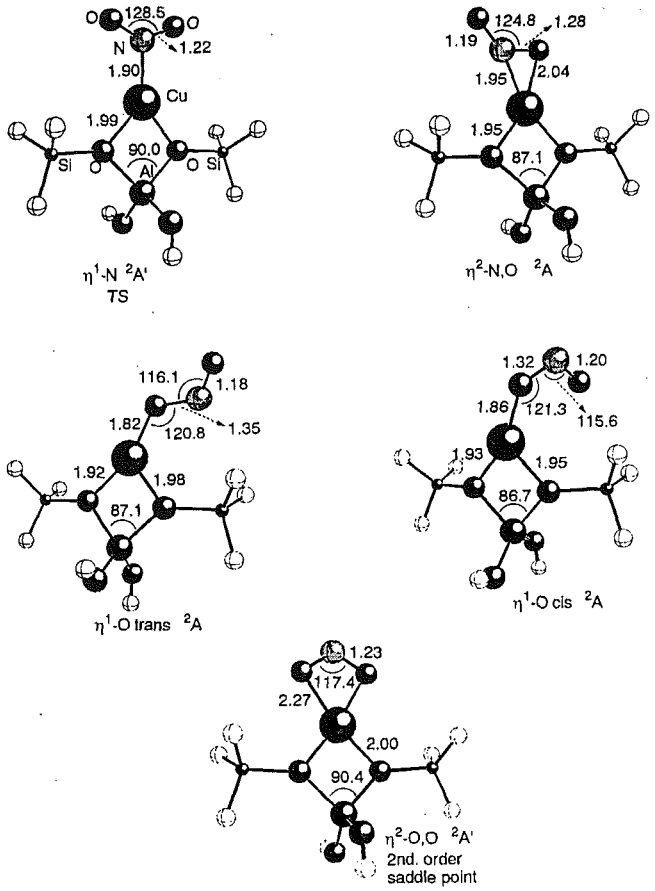

Figure 4. Predicted structures of different isomers of the $ZCuNO_2$ complex ($^2A'$ and ^2A states). The zeolite framework is replaced by the shell-1.5 model in the calculations.

NO_2 to the 4s orbital of Cu and some back-donation from the 3d orbital on Cu to the singly occupied $4b_2$ orbital on NO_2. In effect, there is some 3d−4s promotion (d-population about 9.5, cf. Table 2), and this state can also be described as bonding between Cu^+ (d^9s^1) and the $^2A_1$ state of NO_2.

3.3. Complexes of NO_2 with Cu^+ in Zeolites. Figure 4 shows the structures and Table 1 the binding energies for the complexes of NO_2 with the Cu^+ attached to the zeolite model (CuZ). When coordinated to the zeolite framework, the Cu^+ ion interacts more strongly with NO_2. In general, the distances between Cu and NO_2 are shorter, and the binding energies are larger. Major changes on the topology of the potential energy surfaces occur. The η^1-O minimum structures (cis and trans) and the η^2-O,O transition structure ($^2A_1 - {}^2A'$ states) show the least changes. In the former the binding becomes stronger, while the latter is further destabilized. For the η^2-N,O structure the binding is significantly increased and it becomes a local minimum now, while it was a transition structure in the gas-phase complex. The η^1-N coordination is also stabilized but not as much as the η^2-N,O structure. In the zeolite complex it becomes a transition structure connecting the two symmetrical η^2-N,O minima, while it was a local minimum in the gas-phase complex.

A particular striking case is the $^2B_2$ state of the η^2-O,O complex. In the gas phase it was least binding and an excited state. In the zeolite complex we also find the corresponding state, $^2A''$. However, now it is the most stable one and represents the global minimum. It is four times more stable than the $^2B_2$ state and three times more stable than the $^2A_1$ state of the η^2-O,O complex in the gas phase. Compared with the most strongly bound gas-phase complex (η^1-O trans) the binding energy increases by 62%. To confirm this unusually strong binding effect, we have investigated the η^2-O,O complex of NO_2 by the embedded cluster method. NO_2 was interacting with the quantum part only, but relaxation of the positions of the nuclei of the embedded model was constraint by forces from all the atoms of the periodic zeolite framework. Figure 1a shows the structure found which is virtually identical with that of the complex involving the shell-1.5 model shown in Figure 1b. The binding energy, 42.0 kcal/mol, differs by less than 1 kcal/mol from the result in Table 1. It remains to be seen if this agreement between a free space cluster model which does not represent any specific site and a specific model (T12 site in ZSM-5) persists if additional sites of the MFI framework or different frameworks are considered. If so, there would be an interesting implication: The activation of Cu^+ ions by zeolite frameworks for NO_2 binding is not connected with a particular site in a particular framework. If, e.g., ZSM-5 proves to be a particular efficient Cu-containing catalysts, this may have other reasons than different intrinsic properties of the different $Cu^+[(\equiv SiO)_2Al(O\text{-})_2]^-$ sites.

Before, Yokomichi et al. found that Cu^+ attached to a $(OH)_2Al(OH)_2^-$ model of the zeolite framework binds NO more strongly than the naked Cu^+ ion.[30] The increase was from 38 to 51 kcal/mol—not as large as found here for NO_2.

To analyze the dramatic effect of binding energy increase, we look at the relevant orbitals of NO_2 and ZCu shown in Figure 3. Note that the orbital occupancies shown apply to only one of the different situations discussed below. Z in ZCu stands for the shell-1.5 zeolite model. In the ground state of ZCu the 20a″ orbital is the HOMO of Cu^+ and doubly occupied. This orbital is mainly the d_{xy} orbital of Cu^+ mixed with the $4p_y$ orbital to polarize away from Z^- to reduce repulsion. Thus, the side opposite to the zeolite surface is a high electron density region,

1550 J. Am. Chem. Soc., Vol. 120, No. 7, 1998 Rodriguez-Santiago et al.

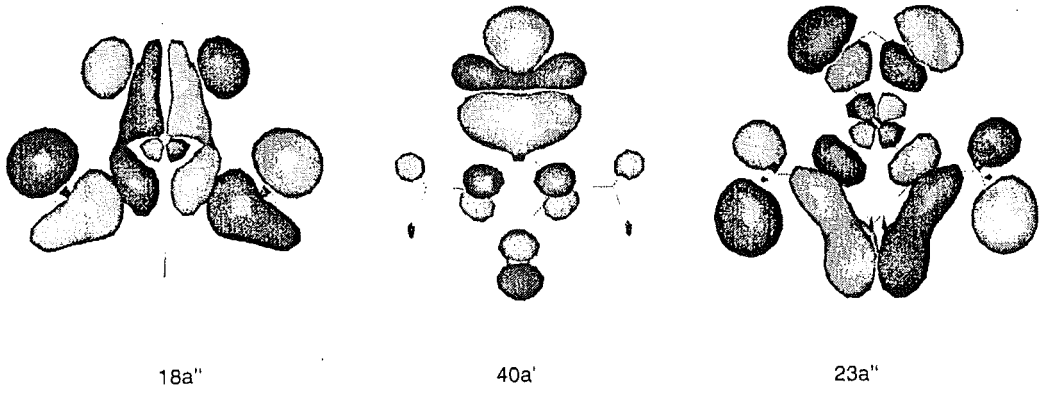

Figure 5. Representation of the 18a", 40a', and 23a" orbitals of the $^2\eta$-O,O isomer of $ZCuNO_2$ in its electronic ground state.

and there is an increased repulsion for the NO_2 ligand approaching the Cu^+ ion on the zeolite wall. The repulsion with all ligands can be reduced by 3d−4s promotion. In the ZCu model this promotion becomes much easier (1.9 eV) than in the naked Cu^+ ion (2.6 eV). We have already seen that the interaction of the naked Cu^+ ion in its d^{10} ground state with NO_2 in its excited $^2B_2$ state results in a 3d−4s promotion. Since this promotion is also facilitated by an increased electrostatic attraction between the Cu^+ ion and the zeolite wall, there is a mutual enhancement. Due to the reduced repulsion between Cu^+ and Z^- in the $^2A''$ state of $ZCuNO_2$, the $Cu^+\cdots O$(zeolite) distances shrink by 0.05 Å on NO_2 bonding, both for the embedded T3 model (Figure 1a) and the nonembedded shell-1.5 model (Figure 1b). This leads to a gain in the electrostatic energy between Cu^+ and Z^-.

We can also start our consideration from the "opposite" situation, NO_2 in its $^2A_1$ ground state and a fully promoted Cu^+ state (d^9s^1). Figure 3 shows the orbital occupancies for this situation. The 36 a' orbital of the ZCu system which was the LUMO in the d^{10} ground state is now singly occupied. This orbital is mainly the 4s orbital of Cu^+. It interacts with the $6a_1$ orbital of NO_2 which is singly occupied in the $^2A_1$ ground state to give a doubly occupied a' orbital (40a', Figure 5). The singly occupied 20a" orbital (d_{xy}) on Cu^+ interacts with the doubly occupied $4b_2$ orbital of NO_2 to yield the singly occupied 23a" orbital above and the doubly occupied 18a" orbital below the 40 a' orbital (Figure 5). Since this three-electron interaction is connected with some donation from the $4b_2$ orbital of NO_2 to the 3d orbital on Cu (20a") and some back-donation from the 4s orbital of Cu^+ to the $6a_1$ orbital of NO_2, the NO_2 gets partially excited and the d^9s^1 state gets less s and more d character. This view is supported by the observation that the structure of the $CuNO_2$ fragment in the $^2A''$ state of the ZCuNO2 complex is very similar to that of the $^2B_2$ state of the η^2-O,O Cu^+NO_2 gas-phase complex (see Figures 1b and 2).

The picture of the bonding is further confirmed by the population analysis given in Table 2. The d occupation on Cu in $ZCuNO_2$ is 9.33—a decrease by 0.52 electrons compared to ZCu. In the gas-phase complex, in which 3d−4s promotion is not enhanced by the Cu^+−zeolite interaction, the 3d population is closer to the d^{10} state, 9.55. Moreover, the Mulliken spin density indicates that the unpaired electron is mainly located on the metal ion since the most important contribution to the singly occupied orbital 23a" comes from the Cu d_{xy} orbital (20a") of ZCu.

The $^2A'$ electronic state of the η^2-O,O $ZCuNO_2$ complex lies 32 kcal/mol above the $^2A''$ ground state. In this case the 40a' orbital is the open shell orbital and the 23a" orbital that is antibonding between ZCu and NO_2 is doubly occupied (Figure 3). Since the Cu contribution to the former is mainly 4s and to the latter mainly 3d (Figure 3), the 3d population in the $^2A'$ state is larger than in $^2A''$, while the 4s population is smaller (Table 2). Figure 3 also shows that the $(18a'')^2(40a')^1(23a'')^2$ occupation corresponds to the orbital occupation in the $^2A_1$ ground state of NO_2. Hence, in the $^2A'$ state of η^2-O,O $ZCuNO_2$ the structure of the $CuNO_2$ fragment is closer to the $^2A_1$ state of gas-phase Cu^+NO_2 than to the $^2B_2$ state (Figure 2 and Table 3). Frequency calculations on the $^2A'$ state show that this stationary point is a second-order saddle point. The movement associated with one of the imaginary frequencies leads to the η^1-O structure (cis), while the other one corresponds to the NO_2 rotation. Since this structure has a very high energy and rotation of NO_2 is not expected to decrease the energy significantly, we have not studied this electronic state further.

For the η^2-N,O coordination the binding energy of the $ZCuNO_2$ complex is twice as large as in the gas phase. The reason is that for this coordination mode the $6a_1$ orbital of NO_2 has the proper local symmetry to interact with the HOMO of ZCu (20a"). The resulting three-electron interaction becomes a more stabilizing two-electron interaction when an electron is promoted from 3d (20a") to 4s (36a'). This 3d−4s promotion on the Cu atom is much larger for ZCu than for Cu for the reasons discussed above. Note that due to reduced repulsion on 3d−4s promotion the $Cu^+\cdots O$ distance shrinks from 1.99 Å in ZCu (Figure 1b) to 1.95 Å in the $ZCuNO_2$ complex (Figure 4). The orbital occupation data of Table 2 support this view. The d population on Cu decreases from 9.85 and 9.83 in ZCu and η^2-N,O Cu^+NO_2, respectively, to 9.43 in η^2-N,O $ZCuNO_2$. The population analysis (Table 2) shows that in Cu^+NO_2 the spin density is mainly located in the NO_2 fragment, while in $ZCuNO_2$ half of the spin is on Cu.

From the above considerations follows that the effect of a largely increased bond strength with Cu^+ in a zeolite is coupled to the presence of a singly occupied orbital available for bonding in the energy region where the Cu orbitals are found. When binding water instead of NO_2 to the CuZ complex, the binding energy calculated for the shell-1.5 model (27 kcal/mol—a similar value has been reported before[15]) decreases compared to the Cu^+OH_2 gas-phase complex energy (43.8 kcal/mol).

To understand if the effect found is specific for zeolites as ligands of Cu^+ or may be also present with other oxygen ligands we have made additional calculations on the $Cu^+(H_2O)_2NO_2$ system (η^2-O,O coordination, $^2B_2$ state). Figure 6 shows the optimized structure. The orbital interactions are the same as in the $^2A''$ state of $ZCuNO_2$, and the structure of the $CuNO_2$ fragment is almost identical (cf. Figures 1 and 6). However, the binding energy computed with respect to the linear equilibrium structure of $Cu^+(H_2O)_2$ is 4.7 kcal/mol only. If it is calculated with the bent structure of $Cu^+(H_2O)_2$ as reference,

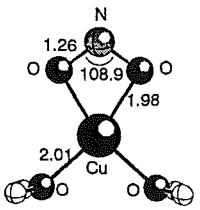

Figure 6. Predicted structure of the $(H_2O)_2Cu^+NO_2$ complex.

i.e., with all structure parameters the same as in the $(H_2O)_2$-Cu^+NO_2 complex, a value of 23.5 kcal/mol is obtained—larger than for the naked Cu^+ ion but still far from that obtained for Cu^+ in zeolites (42.7 kcal/mol). Promotion from d^{10} to d^9s^1 is found as costly (2.6 eV) as for the free Cu^+ ion.

We conclude that half of the activating effect that the zeolite framework has on Cu^+ ions is that it holds the oxygen ligands in the proper position. About the other half is due to the stronger bonding between the negatively charged zeolite surface and the positively charged Cu^+ ion in the presence of NO_2. When 3d–4s promotion reduces repulsion, the zeolite-Cu distance can shrink and there is a gain in electrostatic energy. In contrast, the Cu^+-OH_2 distance is larger in the $(H_2O)_2Cu^+NO_2$ complex (2.02 Å) than in the linear $Cu^+(H_2O)_2$ system (1.98 Å). The Cu^+-OH_2 distance optimized for the bent structure of the $Cu^+(H_2O)_2$ system (O–Cu–O angle fixed to its optimum value in the $(H_2O)_2Cu^+NO_2$ complex) is 2.05 Å. This indicates that with respect to the bent structure as reference there is some reduction of repulsion, but the gain in electrostatic energy (ion–dipole) is not as large as in the $ZCuNO_2$-system (ion-pair interaction).

This has implications for selecting models of the Cu^+ site in zeolites. Although the local structure of the active site of the zeolite and the bonding mechanism can be reasonably well represented by the most simple Cu^+–water models,[25,26,31,32] the unusually strong binding energy of NO_2 (this work) and NO (ref 30) changes significantly from such simple models to the more realistic ones studied in this and previous work (e.g. refs 14,15,28–30).

4. Conclusion

The coordination of Cu^+ to the zeolite framework results in a substantially stronger bonding of NO_2 and in different preferred coordination modes compared to the gas-phase complex between Cu^+ and NO_2. This effect is due to $d^{10}-d^9s^1$ promotion which reduces repulsion with all ligands of Cu^+. As a result orbital interactions between Cu^+ and NO_2 become more favorable and electrostatic interactions between Cu^+ and the negatively charged zeolite wall more attractive. Hence we observe a cooperative (three-body) effect in the system zeolite$^-Cu^+NO_2$ which strengthens both the NO_2-Cu^+ and the Cu^+-zeolite$^-$ interactions.

Acknowledgment. Most calculations for this study have been made when L.R. was at Humboldt-University. Financial support for his stay from the Spanish Minister of Education and Science is gratefully acknowledged. This work has also been supported by the "Fonds der Chemischen Industrie" and by the "Deutsche Forschungsgemeinschaft".

JA973196K

8. Conclusiones

De acuerdo con los objetivos planteados, hemos dividido las conclusiones en dos grandes apartados: a partir del análisis de diferentes métodos de cálculo aplicados al estudio de sistemas metal-ligando podemos extraer las siguientes conclusiones de tipo metodológico:

1. Los métodos del funcional de la densidad proporcionan geometrías y frecuencias vibracionales comparables a las obtenidas con método CCSD(T). Sin embargo, en el cálculo de energías de enlace los resultados son más discrepantes.

2. Las diferencias entre las energías calculadas a nivel DFT y CCSD(T) se han analizado usando los sistemas $ScCO_2$ y $CuNO_2$. En el primer caso, las energías de enlace DFT están sobrestimadas respecto a las energías CCSD(T) debido a la subestimación de la promoción 4s-3d en el Sc^+ por los funcionales actuales. En el sistema $CuNO_2$ las energías de enlace DFT están subestimadas respecto a las energías CCSD(T) debido a la sobrestimación del potencial de ionización del Cu con los funcionales actuales. Estas deficiencias se deben a la descripción incorrecta de los estados atómicos con los funcionales existentes y se solucionan parcialmente introduciendo el intercambio exacto en el funcional.

3. En el complejo $CuNO_2$ la energía de enlace calculada con el método CCSD(T) esta sobrevalorada debido principalmente a la mala descripción del potencial de ionización del Cu. La energía de enlace exacta en este sistema estaría situada entre los valores obtenidos con los métodos del funcional de la densidad y con el método CCSD(T).

4. Los resultados obtenidos con el método QCISD(T) para el sistema $CuNO_2$ son muy diferentes de los obtenidos con el método CCSD(T). En este sistema el método QCISD(T) proporciona resultados incorrectos.

A partir de los resultados obtenidos también se pueden extraer las siguientes conclusiones respecto a la estructura y las propiedades de los diferentes sistemas estudiados:

1. La estructura más estable para el complejo MNO_2 corresponde, en todos los casos estudiados, al NO_2 coordinado al metal a través de los dos oxígenos (coordinación η^2-O,O), que es la coordinación más favorable para la interacción iónica. El estado fundamental en los sistemas con M=Cu y Ag es un estado $^1A_1$. En los sistemas con metales alcalinotérreos el estado fundamental es siempre un estado $^2A_1$ excepto en el caso del Be donde el estado $^2B_1$ es más favorable. Este estado presenta un mecanismo de enlace diferente y es geométricamente muy distinto al del estado $^2A_1$. Todo ello es debido al menor radio atómico del Be.

2. La estructura más estable en el sistema $Cu(NO_2)_2$ es la estructura D_{2h} con los dos fragmentos NO_2 coordinados a través de los dos oxígenos (coordinación η^2-O,O) en el mismo plano con un estado fundamental $^2B_{3g}$. En el sistema $Mg(NO_2)_2$ la estructura D_{2d}, con los dos fragmentos NO_2 en planos perpendiculares, es más estable que la D_{2h}. En este caso el estado fundamental es un $^1A_1$. La mayor estabilidad de la estructura D_{2h} con respecto a la estructura D_{2d} en el caso del $Cu(NO_2)_2$ se debe a la diferente interacción de los orbitales de los ligandos con los orbitales d del metal. En el caso del sistema $Mg(NO_2)_2$ el metal no posee orbitales d ocupados para interaccionar con los ligandos y por tanto el orden de estabilidades se debe únicamente a las diferencias en las interacciones estéricas entre los ligandos.

3. Los valores de los parámetros geométricos optimizados y frecuencias vibracionales calculadas para los fragmentos NO_2, así como el análisis de población muestran que el enlace en los sistemas MNO_2 y $M(NO_2)_2$ estudiados presenta un carácter principalmente iónico tanto en el caso de metales de transición como en el de metales alcalinotérreos.

4. Las frecuencias vibracionales calculadas para los sistemas $CuNO_2$, $CaNO_2$, $SrNO_2$, $Cu(NO_2)_2$ y $Cu(NO_3)_2$ a nivel DFT están en muy buen acuerdo con los datos experimentales existentes.

5. La variación de las energías de enlace en los sistemas MNO_2 está de acuerdo con la presencia de un enlace metal-ligando de tipo básicamente iónico. En particular, el comportamiento de Cu y Mg es muy similar debido a que poseen un primer potencial de ionización muy similar. En los sistemas $M(NO_2)_2$ las energías de enlace totales M-$(NO_2)_2$, y por tanto las del segundo NO_2, $M(NO_2)$-NO_2, muestran importantes diferencias entre $Cu(NO_2)_2$ y $Mg(NO_2)_2$. Dichas diferencias se deben a que el segundo potencial de ionización del Cu es mucho mayor que el del Mg, lo que lleva a una energía de disociación total en el $Cu(NO_2)_2$ menor que en el $Mg(NO_2)_2$.

6. El modo de coordinación del NO_2 al Cu^+ es diferente en el interior de una zeolita, representada por un modelo de *cluster*, que en fase gas. Mientras en fase gas la estructura más estable corresponde al NO_2 coordinado a través de un oxígeno (η^1-O trans), en la zeolita la coordinación más estable es la η^2-O,O con el NO_2 coordinado a través de los dos oxígenos.

7. El mecanismo de enlace del NO_2 también varía cuando se introduce en la zeolita. En el $[CuNO_2]^+$ libre el estado fundamental corresponde a la interacción del estado $^1S(d^{10})$ del Cu^+ con el estado $^2A_1$ del NO_2. Cuando el NO_2 se coordina al Cu^+ en el interior de la zeolita se produce una promoción $3d^{10}$-$3d^9 4s^1$ en el Cu^+ para reducir la repulsión metal-NO_2. A su vez, también se reduce la repulsión entre el Cu^+ y la zeolita con lo que las distancias Cu^+····O(zeolita) se acortan y la interacción electrostática del Cu^+ con la zeolita, cargada negativamente, aumenta.

8. La energía de enlace del NO_2 al Cu^+ en la zeolita, 42.7 kcal mol^{-1}, aumenta considerablemente respecto a la energía de enlace del NO_2 al Cu^+ en fase gas, 26.4 kcal mol^{-1}. Esto se debe al incremento de la atracción entre la superficie de la zeolita y el Cu^+ debido a la promoción 3d-4s en el Cu^+. El análisis del sistema $Cu^+(H_2O)_2NO_2$, donde la zeolita se representa mediante un modelo de moléculas de agua, proporciona

una energía de enlace del NO_2 de 23.5 kcal mol^{-1}. Por tanto, ni el Cu^+ aislado, ni el modelo de moléculas de agua representan correctamente la adsorción del NO_2 en la zeolita CuZSM-5.

9. La inclusión del efecto de toda la zeolita mediante un método que combina la mecánica cuántica y la mecánica molecular no produce cambios apreciables respecto a la geometría y a la energía de enlace obtenidas con el modelo de *cluster* para la coordinación más estable. Por tanto, el modelo que hemos utilizado parece, en principio, un buen modelo para continuar con el estudio del mecanismo de la descomposición de los óxidos de nitrógeno.

9. Referencias

[1] Hitchman, M. A.; Rowbottom,G. L. *Coord. Chem. Rev.* **1982**, *42*, 55.

[2] Hathaway, B. J. In *Comprehensive Coordination Chemistry*; Pergamon: London, 1987; vol 2, p 413.

[3] Birdy, R.; Goodgame, D. M. L.; McConway, J. C.; Rogers, D. *J. Chem. Soc. Dalton Trans.*, **1977**, 1730.

[4] Luke Hart, C. M.; Troup, J. M. *Inorg. Chim. Acta*, **1977**, *22,* 81.

[5] Minacheva, L. Kh.; Porai-Koshits, M. A.; Antsyshkina, A. S. *Russ. J. Struct. Chem.*, **1969**, *10* 72.

[6] Drew, M. G. D.; Goodgame, D. M. L.; Hitchman, M. A.; Rogers, D. *Proc. Chem. Soc*, **1964**, 363.

[7] Ham, D. O.; Kinsey, J. L.; *J. Chem. Phys.* **1968**, *48*, 939.

[8] Herm, R. R.; Herschbach, D. R. *J. Chem. Phys.*, **1970**, *52*, 5783.

[9] Ham, D. O.; Kinsey, J. L. *J. Chem. Phys.* **1970**, *53*, 285.

[10] Milligan, D. E.; Jacox, M. *J. Chem. Phys.* **1971**, *55*, 3404.

[11] Parrish, D. D.; Herm, R. R. *J. Chem. Phys* **1971**, *54*, 2518.

[12] Barbeschi, M.; Bencivenni, L.; Ramondo, F. *Chem. Phys.* **1987**, *112*, 387.

[13] W.-J. Lo; M.-y., Shen; C.-h., Yu; Y.-P., Lee *J. Chem. Phys.***1996**, *104*, 935.

[14] Herm, R. R.; Lin, S.-M.; Mims, C. A. *J. Phys. Chem.* **1973**, *77*, 2931.

[15] Tevault, D. E.; Andrews, L. *Chem. Phys. Lett.*, **1977**, *48*, 103.

[16] Cox, J. W.; Dagdigian, P. J. *J. Chem. Phys* **1983**, *79*, 5351.

[17] Suits, A. G.; Hou, H.; Davis, H. F; Lee, Y. T. *J. Chem. Phys*, **1992**, *96*, 2772.

[18] Davis, H. F.; Suits, A. G.; Lee, Y. T. *J. Chem. Phys.* **1992**, *96*, 6710

[19] Cheong, B. S.; Parson, J. M. *J. Chem. Phys.* **1994**, *100*, 2637.

[20] Worden, D.; Ball, D. W. *J. Phys. Chem.* **1992**, *96*, 7167.

[21] Vinckier, C.; Verhaeghe, T.; Vanhees, I. *J. Chem. Soc. Faraday Trans.* **1994**, *90*, 2003.

[22] (a) *Denitrification, Nitrification, and Atmospheric Nitrous Oxide*; Delwiche, C. C., Ed.; John Wiley & Sons: New York, 1981.(b) Payne, W. J. In *Denitrification*; John Wiley & Sons: New York, 1981.

[23] Komeda, N; Nagao, H.; Adachi, G.-y.; Suzuki, M.; Uehara, A.; Tanaka, K. *Chem. Let.* **1993**, 1521.

[24] Shelef, M; *Chem. Rev.* **1995**, *95*, 209.

[25] *Nitrogen oxides*; Graham, J. A.; Grant, L. D.; Folinsbee, L. J.; Kotchmar, D. J.; Garner, J. H. B., Ed; World Health Organization: Geneva, 1997.

[26] Bosch, H.; Janssen, F. *Catal. Today* **1987**, *2*, 1.

[27] Iwamoto, M.; Mizuno, N. *J. Automot. Eng. (part D Proc. Inst. Mech. Eng.)* **1993**, *207*, 23.

[28] Iwamoto, M.; Furukawa, H.; Mine, Y.; Uemura, F.; Mikuriya, S.-i.; Kagawa, S. *J. Chem. Soc., Chem. Commun.* **1986**, 1273.

[29] Crucq, A.; Frennet, A. In *Catalysis and Automotive Pollution Control*; Elsevier: Amsterdam, 1987; p 1.

[30] Harrison, B.; Wyatt, M.; Gough, K. G. In *Catalysis*; Royal Society of Chemistry: London, 1982; Vol 5, p127.

[31] Meier, W. M.; Olson, D. H. *Atlas of Zeolite Structure Types*; Butterworths: London, 1992.

[32] Thomas, J. M. *Sci. Am.* **1992**, *266*(4), 82.

[33] Olson, D. H.; Kokotailo, G. T.; Lawton, S. L.; Meier, W. M. *J. Phys. Chem.* **1981**, *85*, 2238.

[34] van Koningsveld, H.; Jansen, J. C.; van Bekkum, H. *Zeolites* **1990**, *10*, 235.

[35] Derouane, E. G.; Fripiat, J. G. Zeolites **1985**, *5* 165.

[36] Swaisgood, A. A.; Barr, M. K.; Hay, P. J.; Redondo, A. *J. Phys. Chem.* **1991**, *96*, 10031.

[37] Chatterjee, A.; Vetrivel, R.; *Zeolites* **1994** *14* 225.

[38] Blanco, F.; Villalba, G. U.; Agudelo, M. M. R. *Mol. Simul.* **1995**, *14*, 165.

[39] Schröeder, K.-P.; Sauer, J.; Leslie, M.; Catlow, C. R. A. *Zeolites* **1992**, *12*, 20.

[40] Valyon, J.; Hall, W. K. *J. Catal.* **1993**, *143*, 520.

[41] Valyon, J.; Millman, W. S.; Hall, W. K. *Catal. Lett.* **1994**, *24*, 215.

[42] Beutel, T.; Sárkány, J.; Lei, G.-D.; Yan, J. Y.; Sachtler, W. M. H. *J. Phys. Chem.* **1996**, *100*, 845.

[43] Iwamoto, M.; Yahiro, H.; Tanda, K.; Mizuno, N.; Mine, Y.; Kagawa, S. *J. Phys. Chem.* **1991**, *95*, 3727.

[44] Jang, H.-J.; Hall, W. K.; d'Itri, J. L. *J. Phys. Chem.* **1996**, *100*, 9416.

[45] Li, Y.; Hall, W. K. *J. Catal.* **1991**, *129*, 202.

[46] Liu, D.-J.; Robota, H. J. *Catal. Lett.* **1993**, *21*, 291.

[47] Larsen, S. C.; Aylor, A.; Bell, A. T.; Reimer, J. A. *J. Phys. Chem.* **1994**, *98*, 11533.

[48] Yamashita, H.; Matsuoka, M.; Tsuji, K.; Shioya, Y.; Anpo, M.; Che, M. *J. Phys. Chem.* **1996**, *100*, 397.

[49] Lamberti, C.; Bordiga, S.; Salvalaggio, M.; Spoto, G.; Zecchina, A.; Geobaldo, F.; Vlaic, G.; Bellatreccia, M. *J. Phys. Chem. B* **1997**, *101*, 344.

[50] Spoto, G.; Bordiga, S.; Ricchiardi, G.; Scarano, D.; Zecchina, A.; Geobaldo, F. *J. Chem. Soc., Faraday Trans.* **1995**, *91*, 3285.

[51] Spoto, G.; Bordiga, S.; Scarano, D.; Zecchina, A. *Catal. Lett.* **1992**, *13*, 39.

[52] Liu, D.-J.; Robota, H. J. *Appl. Catal B* **1994**, *4*, 155.

[53] Spoto, G.; Zecchina, A.; Bordiga, S.; Ricchiardi, G.; Martra, G. *Appl. Catal. B* **1994**, *3*, 151.

[54] Grünert, W.; Hayes, N. W.; Joyner, R. W.; Shpiro, E. S.; Siddiqui, M. R. H.; Baeva, G. N. *J. Phys. Chem.* **1994**, *98*, 10832.

[55] Kuroda, Y.; Yoshikawa, Y.; Konno, S.; Hamano, H.; Maeda, H.; Kumashiro, R.; Nagao, M. *J. Phys. Chem.* **1995**, *99*, 10621.

[56] Hamada, H.; Matsubayashi, N.; Shimada, H.; Kintaichi, Y.; Ito, T.; Nishijima, A. *Catal. Lett.* **1990**, *5*, 189.

[57] Giamello, E.; Murphy, D.; Magnacca, G.; Morterra, C.; Shioya, Y.; Nomura, T.; Anpo, M *J. Catal.* **1992**, *136*, 510.

[58] Shelef, M. *Catal. Lett.* **1992**, *15*, 305.

[59] Valyon, J.; Hall, W. K. *J. Phys. Chem.* **1993**, *97*, 1204.

[60] Hamada, H.; Kintaichi, Y.; Sasaki, M.; Ito, T.; *Appl. Catal.* **1991**, *70*, L15.

[61] Shelef, M.; Montreuil, C. N.; Jen, H.-W. *Catal. Lett.* **1994**, *26*, 277.

[62] Tabata, T.; Ohtska, H.; Kokitsu, M; Okada, O. *Bull. Chem. Soc. Jpn.* **1995**, *68*, 1905.

[63] Adelman, B. T.; Beutel, T.; Lei, G.-D.; Sachtler, W. M. H. *J. Catal.* **1996**, *158*, 327.

[64] Goddard, J. D.; Klein, M. L. *Phys. Rev. A* **1983**, *28*, 1141.

[65] Ramondo, F. *Chem. phys. Lett.* **1989**, *156*, 346.

[66] Ramondo, F.; Bencivenni, L.; Sanna, N.; Nunziante Cesaro, S. *J. Mol. Struct. (Theochem)* **1992**, *253*, 121.

[67] Sayle, D. C.; Perrin, M. A.; Nortier, P.; Catlow, C. R. A. *J. Chem. Soc., Chem. Commun.* **1995**, ,945.

[68] Sayle, D. C.; Catlow, C. R. A.; Gale, J. D.; Perrin, M. A.; Nortier, P. *J. Phys. Chem. A* **1997**, *101*, 3331.

[69] Blint, R. J. *J. Phys. Chem.* **1996**, *100*, 19518.

[70] Teraischi, K.; Ishida, M.; Irisawa, J.; Kume, M.; Takahashi, Y.; Nakano, T.; Nakamura, H.; Miyamoto, A. *J. Phys. Chem. B* **1997**, *101*, 8079.

[71] Schneider, W. F.; Hass, K. C. *J. Phys. Chem.* **1996**, *100*, 6032.

[72] Hass, K. C.; Schneider, W. F. *J. Phys. Chem.* **1996**, *100*, 9292.

[73] Ramprasad, R.; Schneider, W. F.; Hass, K. C.; Adams, J. B. *J. Phys. Chem. B* **1997**, *101*, 1940.

[74] Schneider, W. F.; Hass, K. C.; Ramprasad, R.; Adams, J. B. *J. Phys. Chem. B* **1997**, *101*, 4353.

[75] Ramprasad, R.; Hass, K. C.; Schneider, W. F.; Adams, J. B. *J. Phys. Chem. B* **1997**, *101*, 6903.

[76] Brand, H. V.; Redondo, A.; Hay, P. J. *J. Phys. Chem. B* **1997**, *101*, 7691.

[77] Yokomichi, Y.; Ohtsuka, H.; Tabata, T.; Okada, O.; Yokoi, Y.; Ishikawa, H.; Yamaguchi, R.; Matsui, H.; Tachibana, A.; Yamabe, T. *Cat. Today* **1995**, *23*, 431.

[78] Yokomichi, Y.; Yamabe, T.; Ohtsuka, H.; Kakumoto, T. *J. Phys. Chem.* **1996**, *100*, 14424.

[79] Trout, B. L.; Chakraborty, A. K.; Bell, A. T. *J. Phys. Chem.* **1996**, *100*, 4173.

[80] Trout, B. L.; Chakraborty, A. K.; Bell, A. T. *J. Phys. Chem.* **1996**, *100*, 17582.

[81] Hartree, D. R. *Proc. Cambridge Phil. Soc.* **1928**, *24*, 89.

[82] Fock, V. *Z. Physik* **1939**, *61*, 126.

[83] Bartlett, R. J. *Ann. Rev. Phys. Chem.* **1981**, *32*, 359.

[84] Freed, K. F. *Ann. Rev. Phys. Chem.* **1971**, *22*, 313.

[85] Löwdin, P. O. In *Perturbation Theory and its Application in Quantum Mechanics*; Wilcox, L. H. Ed.; Wiley: New York, 1966.

[86] Löwdin, P. O. *Int. J. Quant. Chem.* **1968**, *2*, 867.

[87] Bueckner, K. A. *Phys. Rev.* **1953**, *97*, 1353.

[88] Goldstone, J. *Proc. Roy. Soc.* **1952**, *A293*, 267.

[89] Møller, C.; Plesset, M. S. *Phys. Rev.* **1934**, *46*, 618.

[90] Shavitt, I. In *Modern Theoretical Chemistry, 3*; Schaefer III, H. F. Ed; New York, 1977.

[91] Roos, B. *Chem Phys. Lett.*, **1972**, *15*, 153.

[92] Knowles, P. J.; Handy, N. C. *Chem. Phys. Lett.* **1984**, *111*, 315.

[93] Pople, J. A.; Head-Gordon, M.; Raghavachari, K. *J. Chem. Phys.*, **1987**, *87*, 5968.

[94] Alrichs, R.; Scharf, P.; Ehrhardt, C. *J. Chem. Phys.* **1984**, *82*, 890.

[95] Chong, D. P.; Langhoff, S. R. *J. Chem. Phys.* **1986**, *84*, 5606.

[96] Cizek, J. *J. Chem. Phys.* **1966**, *45*, 4256.

[97] Purvis, G. D.; Bartlett, R. J. *J. Chem. Phys.* **1982**, *76*, 1910.

[98] Raghavachari, K.; Trucks, G. W.; Pople, J. A.; Head-Gordon, M. *Chem. Phys. Lett.* **1989**, *157*, 479.

[99] Hohenberg, P.; Kohn, W. *Phys. Rev. B* **1964**, *136*, 864.

[100] Kohn, W.; Sham, L. J. *Phys. Rev. A* **1965**, *140*, 1133.

[101] Vosko, S. J.; Wilk, L.; Nusair, M. *Can. J. Phys.* **1980**, *58*, 1200.

[102] Becke, A. D. *Phys. Rev. A* **1988**, *38*, 3098.

[103] Perdew, J. P. *Phys. Rev. B* **1986**, *33*, 8822.

[104] Perdew, J. P. In *Electronic Structure of Solids '91*, Ziesche, P.; Eschring, H. Ed.; Akademie: Berlin, 1991; Perdwe, J. P.; Chevary, J. A.; Vosko, S. H.; Jackson, K. A.; Pederson, M. R.; Singh, D. J.; Fiolhais, C. *Phys. Rev. B* **1992**, *46*, 6671. Perdew, J. P.; Wang, Y. (unpublished).

[105] Lee, C.; Yang, W.; Parr, R. G. *Phys. Rev. B*, **1988**, *37*, 785.

[106] Becke, A. D. *J. Chem. Phys.* **1993**, *98*, 1372.

[107] Becke, A. D. *J. Chem. Phys.* **1993**, *98*, 5648.

[108] Eichler, U.; Kölmel, C. M.; Sauer, J. *J. Comput. Chem.* **1996**, *18*, 463.

[109] Singh, U. C.; Kollman, P. A.; *J. Comput. Chem.* **1986**, *7*, 718.

[110] Field, M. J.; Bash, P. A.; Karplus, M. *J. Comput. Chem.* **1990**, *11*, 700.

[111] Stanton, R. V.; Hartsough, D. S.; Merz Jr., K. M. *J. Phys. Chem.* **1993**, *97*, 11868.

[112] Stanton, R. V.; Hartsough, D. S.; Merz Jr., K. M. *J. Comput. Chem.* **1995**, *16*, 113.

[113] Maseras, F.; Morokuma, K. *J. Comput. Chem.* **1995**, *16*, 1170.

[114] Warshel, A. *Computer Modelling of Chemical Reactions in Enzymes and Solutions*; John Wiley & Sons: New York, 1991.

[115] *Modelling of Structure and Reactivity in Zeolites*; Catlow, C. R. A. Ed.;Academic: London, 1992.

[116] Dick, B. G.; Overhauser, A. W. *Phys. Rev.* **1958**, *112*, 90.

[117] Böhme, M.; Frenking, G. *Chem. Phys. Letters* **1994**, *224*, 194.

[118] Fournier, R. *J. Chem. Phys.* **1993**, *98*, 8041.

[119] Fournier, R. *J. Chem. Phys.* **1993**, *99*, 1801.

[120] Pápai, I.; Mink, J.; Fournier, R.; Salahub, D. R. *J. Phys. Chem.* **1993**, *97*, 9986.

[121] Ziegler, T.; Li, J. *Can. J. Chem.* **1994**, *72*, 783.

[122] Castro, M.; Salahub, D. R.; Fournier, R. *J. Chem. Phys.* **1994**, *100*, 8233.

[123] Barone, V. *Chem. Phys. Lett.* **1995**, *233*, 129.

[124] Ricca, .A; Bauschlicher, C. W. *Theor. Chim. Acta* **1995**, *92*, 123.

[125] Bauschlicher, C. W.; Maitre, P. *J. Phys. Chem.* **1995**, *99*, 3444.

[126] Maitre, P.; Bauschlicher, C. W. *J. Phys. Chem.* **1995**, *99*, 6836.

[127] Holthausen, M. C.; Heinemann, C.; Cornehl, H. H.; Koch, W.; Schwarz, H. *J. Chem. Phys.* **1995**, *102*, 4931.

[128] Holthausen, M. C.; Mohr, M.; Koch, W. *Chem. Phys. Lett.* **1995**, *240*, 245.

[129] Pápai, I. *J. Chem. Phys.* **1995**, *103*, 1860.

[130] Ricca, .A; Bauschlicher, C. W. *Chem. Phys. Lett.* **1995**, *245*, 150.

[131] Fournier, R.; Pápai, I. In *Recent Advances in Density Functional Methods, Vol. 3 Applications*; Chong, D., Ed; World Scientific: Singapore, 1995.

[132] Chung, S. C.; Krüger, G.; Pacchioni, G.; Rösch, N. *J. Chem. Phys.* **1995**, *102*, 3695.

[133] Terra, J.; Guenzburger, D. *J. Phys. Chem.* **1995**, *99*, 4953.

[134] Chung, S. C.; Krüger, G.; Ruzankin, S. P.; Pacchioni, G.; Rösch, N. *Chem. Phys. Lett.* **1996**, *248*, 109.

[135] Scott, A. P.; Radom, L. *J. Phys. Chem.* **1996**, *100*, 16502.

[136] Gunnarsson, O.; Jones, R. O. *Phys. Rev. B* **1985**, *31*, 7588.

[137] Russo, T. V:; Martin, R. L.; Hay, P. J. *J. Chem. Phys.* **1994**, *101*, 7729.

[138] Kutzler, F. W.; Painter, G. S. *Phys. Rev. B* **1991**, *43*, 6865.

[139] Raghavachari, K.; Trucks, G. W. *J. Chem. Phys.* **1989**, *91*, 2457.

[140] Moore, C. E. In *Atomic Energy Levels*; Natl. Bur. Stand. (US) circ. 467: 1949.

[141] La Villa, R. E.; Bauer, S. H. *J. Am. Chem. Soc.* **1963**, *85*, 3597.

[142] Rossi, V.; Sadun, C.; Bencivenni, L.; Caminiti, R. *J. Mol. Struct. (Theochem)* **1994**, *314*, 247.